FEDERAL UNIVERSITY OF TECHNOLOGY - PARANÁ
GRADUATE PROGRAM IN ELECTRICAL AND COMPUTER ENGINEERING (CPGEI)

THIAGO DE QUADROS

# DEVELOPMENT AND EVALUATION OF AN ELDERLY FALL DETECTION SYSTEM BASED ON A WEARABLE DEVICE LOCATED AT WRIST

DISSERTATION

**CURITIBA**

**2017**

THIAGO DE QUADROS

# DEVELOPMENT AND EVALUATION OF AN ELDERLY FALL DETECTION SYSTEM BASED ON A WEARABLE DEVICE LOCATED AT WRIST

Dissertation presented to the Graduate Program in Electrical and Computer Engineering (CPGEI) at Federal University of Technology - Paraná as partial requirement to obtain a "Master of Science" degree – Area: Biomedical Engineering.

Supervisor: Prof. Dr. Fabio K. Schneider

Co-supervisor: Prof. Dr. André E. Lazzaretti

**CURITIBA**

**2017**

**Dados Internacionais de Catalogação na Publicação**

Q1d 2017

Quadros, Thiago de
Development and evaluation of an elderly fall detection system based on a wearable device located at wrist = Desenvolvimento e avaliação de um sistema de detecção de quedas de idosos baseado em um dispositivo vestível localizado no punho / Thiago de Quadros.-- 2017.
86 f.: il.; 30 cm.

Disponível também via World Wide Web.
Texto em inglês, com resumo em português.
Dissertação (Mestrado) - Universidade Tecnológica Federal do Paraná. Programa de Pós-Graduação em Engenharia Elétrica e informática Industrial, Curitiba. Área de Concentração: Engenharia Biomédica, 2017.
Bibliografia: f. 81-86.

1. Quedas (Acidentes) em idosos - Prevenção. 2. Detecção de sinais. 3. Aprendizado do computador. 4. Processamento de sinais - Técnicas digitais. 5. Algoritmos computacionais. 6. Processamento eletrônico de dados em tempo real. 7. Métodos de simulação. 8. Instrumentos e aparelhos médicos. 9. Engenharia biomédica. 10. Engenharia elétrica - Dissertações. I. Schneider, Fábio Kurt, orient. II. Lazzaretti, André Eugênio, coorient. III. Universidade Tecnológica Federal do Paraná. Programa de Pós-Graduação em Engenharia Elétrica e Informática Industrial. IV. Desenvolvimento e avaliação de um sistema de detecção de quedas de idosos baseado em um dispositivo vestível localizado no punho.

CDD: Ed. 22 -- 621.3

**Biblioteca Central do Câmpus Curitiba - UTFPR**

Ministério da Educação
Universidade Tecnológica Federal do Paraná
Diretoria de Pesquisa e Pós-Graduação

# TERMO DE APROVAÇÃO DE DISSERTAÇÃO Nº____

A Dissertação de Mestrado intitulada **"Development and evaluation of an Elderly Fall Detection System Based on Wearable Device Located at Wrist"** defendida em sessão pública pelo(a) candidato(a) **Thiago de Quadros**, no dia 31 de agosto de 2017, foi julgada para a obtenção do título de Mestre em Ciências, área de concentração Engenharia Biomédica, e aprovada em sua forma final, pelo Programa de Pós-Graduação em Engenharia Elétrica e Informática Industrial

BANCA EXAMINADORA:

Prof(a). Dr(a). Joaquim Miguel Maia - Presidente – (UTFPR)
Prof(a). Dr(a). André Eugênio Lazzaretti - (UTFPR)
Prof(a). Dr(a). Rodrigo Jardim Riella – (LACTEC)

A via original deste documento encontra-se arquivada na Secretaria do Programa, contendo a assinatura da Coordenação após a entrega da versão corrigida do trabalho.

Curitiba, 31 de agosto de 2017.

This work is dedicated to my family and friends, who have continuously encouraged me to make a difference in society.

## ACKNOWLEDGMENTS

There are many people related to this work's development who I would like to thank.

God, who gave me a passion for science and love for helping, the two fundamental forces for this work's development.

My family, for all the support and encouragement to complete this additional step in my professional journey.

My wife Andressa, who tolerated all my long absences due to the time spent in this project, and for supporting me with love from the beginning to the end of this work.

My brother Matheus, who helped me with text revisions which allowed me to improve the clarity of this dissertation.

André Lazzaretti, for all the help, orientation and encouragement. His participation was fundamental to this work's development. Also, he was always available to help, from sunny Monday mornings to rainy Sunday evenings.

Fabio Schneider, for guiding me during all this academic step, patiently helping me to become a better engineer and researcher.

Leonardo Silveira, for the English revision. His help removes the geographical boundaries of this work.

And many other friends and work colleagues, who helped me with suggestions, experiences or encouragement.

The secret of getting ahead is getting started. - Mark Twain

# ABSTRACT

QUADROS, Thiago de. DEVELOPMENT AND EVALUATION OF AN ELDERLY FALL DETECTION SYSTEM BASED ON A WEARABLE DEVICE LOCATED AT WRIST. 88 p. Dissertation – Graduate Program in Electrical and Computer Engineering (CPGEI), Federal University of Technology - Paraná. Curitiba, 2017.

Falls in the elderly age are a world health problem. Every year, about 30% of people aged 65 or older become victims of fall events. The consequences of a fall may be physiological (e.g. bone fractures, muscular injuries) and psychological, including the loss of self-confidence by fear of falling, which leads to new falls. A solution to this problem is related to preventive actions (e.g. adapting furniture) allied to fall detection systems, which can alert family members and emergency medical services. Since the response time for help is related to the fall's consequences and severity, such systems must offer high accuracy and real-time fall detection. Although there are many fall detection solutions in literature (most part of them related to wearable devices), few of them are related to wrist-worn devices, mainly because of the existing challenges for this configuration. Considering the wrist as a comfortable, discrete and acceptable place for an elderly wearable device (less associated to the stigma of using a medical device), this work proposes the development and evaluation of a fall detection solution based on this configuration. For this, different sensors (accelerometer, gyroscope and magnetometer) were combined to different algorithms, based on threshold and machine learning methods, in order to define the best signals and approach for an elderly fall detection. These methods considered acceleration, velocity and displacement information, relating them with wrist spatial orientation, allowing the calculation of the vertical components of each movement. For the algorithms' training and evaluation, two different protocols were employed: one involving 2 volunteers (both males, ages of 27 and 31) performing a total of 80 fall and 80 non-fall events simulation, and the other involving 22 volunteers (14/8 males/females, ages mean: $25.2 \pm 4.7$) performing a total of 396 fall and 396 non-fall events simulation. An exhaustive evaluation of different signals and configuration parameters was performed for each method. The best threshold-based algorithm employed the vertical acceleration and total velocity signals, achieving 95.8% and 86.5% of sensitivity and specificity, respectively. On the other hand, the best machine learning algorithm was based on the K-Nearest Neighbors method employing the vertical acceleration, velocity and displacement information combined with spatial orientation angles: 100% of sensitivity and 97.9% of specificity. The obtained results allow to emphasize the relevance of machine learning algorithms for wrist-worn fall detection systems instead of traditional threshold-based algorithms. These results offer great contributions for the research of similar wearable fall detectors, suggesting the best approach for new developments.

**Keywords:** Fall Detection, Machine Learning, Threshold-based Methods.

# RESUMO

QUADROS, Thiago de. DESENVOLVIMENTO E AVALIAÇÃO DE UM SISTEMA DE DETECÇÃO DE QUEDAS DE IDOSOS BASEADO EM UM DISPOSITIVO VESTÍVEL LOCALIZADO NO PUNHO. 88 f. Dissertation – Graduate Program in Electrical and Computer Engineering (CPGEI), Federal University of Technology - Paraná. Curitiba, 2017.

A queda de idosos é um problema de saúde mundial. Todos os anos, cerca de 30% dos idosos com 65 anos ou mais são vítimas de quedas. Além disso, as consequências de uma queda podem ser fisiológicas (e.g. fraturas ósseas, ferimentos musculares) e psicológicas, como a perda de autoconfiança, levando a novas quedas. Uma solução para este problema está relacionada com ações preventivas (e.g. adaptação de mobília) aliadas a sistemas de detecção de quedas, os quais podem notificar familiares e serviços médicos de urgência. Como o tempo de espera por socorro após uma queda está relacionado com a severidade das consequências dela, esses sistemas devem oferecer elevada acurácia e detecção em tempo real. Embora existam várias soluções para isso na literatura (a maioria relacionada com dispositivos vestíveis), poucas delas estão relacionadas a dispositivos de punho, principalmente por causa dos desafios existentes para essa configuração. Considerando o punho como um local mais confortável, discreto e aceitável para uso de um dispositivo (menos associado com o estigma do uso de uma solução médica), este trabalho propõe o desenvolvimento e avaliação de uma solução baseada nessa configuração. Para isso, diferentes sensores (acelerômetro, giroscópio e magnetômetro) foram combinados com diferentes algoritmos, baseados em métodos de limiar e aprendizado de máquina, visando definir os melhores sinais e abordagem para a detecção de quedas. Esses métodos consideraram informações de aceleração, velocidade, deslocamento e orientação espacial, permitindo o cálculo de componentes verticais do movimento. Para o treino e avaliação dos algoritmos, dois protocolos diferentes foram empregados: um primeiro envolvendo 2 voluntários (homens, 27 e 31 anos) simulando um total de 80 sinais de queda e 80 de não-queda, e um segundo envolvendo 22 voluntários (14/8 homens/mulheres, idade média: 25,2 $\pm$ 4,7) simulando um total de 396 sinais de queda e 396 de não-queda. Uma análise exaustiva de diferentes sinais e parâmetros de configuração foi executada para cada método. O melhor algoritmo baseado em limiar considerou sinais de aceleração vertical e velocidade total, alcançando 95,8% de sensibilidade e 86,5% de especificidade. Por outro lado, o melhor algoritmo de aprendizagem de máquina foi o baseado no método K-Nearest Neighbors, considerando informações de aceleração, velocidade e deslocamento verticais combinadas com os ângulos de orientação espacial: 100% de sensibilidade e 97,9% de especificidade. Os resultados obtidos permitem enfatizar a relevância de algoritmos de aprendizagem de máquina para sistemas de detecção de queda vestíveis localizados no punho quando comparados a algoritmos baseados em limiar. Esta conclusão oferece grande contribuição para a pesquisa de detectores de quedas similares, sugerindo a melhor abordagem para novos desenvolvimentos.

**Palavras-chave:** Detecção de Quedas, Aprendizado de Máquina, Métodos de Limiarização.

## LIST OF FIGURES

## LIST OF TABLES

## LIST OF ABBREVIATIONS

| | |
|---|---|
| ADL | Activities of daily life |
| ATWI | Acceleration time-window integration |
| CEP | Research Ethics Comittee |
| HMM | Hidden Markov Model |
| IMU | Inertial Measurement Unity |
| LDA | Linear Discriminant Analysis |
| LSOA | Limit for spatial orientation by acceleration |
| RMS | Root mean square |
| SUS | *Serviço Único de Saúde* (Brazilian Public Health System) |
| SVM | Support vector Machine |
| TA | Total acceleration |
| TD | Total displacement |
| TV | Total velocity |
| TWAM | Time-window for acceleration magnitude |
| VA | Vertical acceleration |
| VD | Vertical displacement |
| VTWI | Velocity time-window integration |
| VV | Vertical velocity |

## LIST OF SYMBOLS

| | |
|---|---|
| $\phi$ | Rotation angle over x axis, also known as roll |
| $\theta$ | Rotation angle over y axis, also known as pitch |
| $\psi$ | Rotation angle over z axis, also known as yaw |
| $\alpha$ | Rotation angle associated to the unit quaternion |
| $\upsilon$ | Unit vector associated to the unit quaternion |
| $w_f$ | Size of the low-pass filter time window |
| $w_i$ | Size of the integration time window |

**SUMMARY**

# 1 INTRODUCTION

The average age of the world population is increasing. According to the United Nations 2015 Report for World Population Ageing, between 2015 and 2030, the number of people aged 60 years old and over is expected to grow by 56 percent (UNITED NATIONS, 2015). A World Health Organization report also identified that a child born in Brazil in 2015 is expected to live 20 years longer than any child born 50 years before (WHO, 2015), reinforcing the concept of world people ageing. For reasons like these, problems related to elderly life quality have become a mainstream topic for technology companies that previously presented solutions mainly for young people.

Related to the medical area, different solutions associated to decentralized health systems have been developed to provide, through home health care devices, improved comfort and independence to the elderly. Thus, these solutions have become more and more relevant, encouraging new researches and developments (KHAN; HOEY, 2016).

One of the most severe problems faced by elderly people is the risk of falling. From 28% to 35% of people over the age of 65 fall every single year (WHO, 2007). This number is even bigger when they are over the age of 70, reaching 32% to 42%. Furthermore, the fall recurrence is also a worrisome fact. Tinetti et al. (1988), investigating elder people from a community, observed an alarming fact: for every three elderly victims of a fall, two of them would suffer a new fall in six months. Similarly, Sri-on et al. (2017) evaluated the data from emergency department visitors, identifying that 22.6% of the elderly fall victims suffered at least one new fall in six months. This recurrence is also strengthened by psychological reasons. The fear of falling and low confidence reduces elderly mobility, leading to a low life's quality, and increased risk of falling (ASCHKENASY; ROTHENHAUS, 2006).

About the consequences caused by falls in the elderly, a proper analysis can separate it into three different categories: the consequences for the victim, the consequences for the family and friends and the consequences for the public health system.

As mentioned before, every fall suffered by an elder person directly increases the risk

of a new fall, both for psychological reasons and physiological damages. Since in older age the human body is not so strong and robust as in youth, bone fractures and muscle injuries are popular consequences of falls, requiring weeks or months for a proper recovery. Combining these consequences with the fear of falling and the low confidence, the elderly quality of life is strongly affected, normally related to a loss of independence (AL-AAMA, 2011).

Associated to the consequences above, the family and friends' support is important for elderly recovery. However, as this situation normally affects their routine (requiring their participation on elderly treatment and daily routine), some psychological negative effects are also seen in fall victims' family and friends. Worry and anxiety are common in these cases, leading to attempts of controlling elderly living that reduce its quality (WHO, 2015).

Finally, falls in elderly age are responsible for a high cost of public health systems. The average cost for every hospitalization related to fall injuries ranges from US$6646 on Ireland to US$17483 on USA (WHO, 2007). In Brazil, it is estimated that more than R$160 million were spent in 2015 with treatments of fractures related to elderly falls (DATASUS, 2015). Beyond these direct costs, indirect ones like productivity loss of family and debt due to health expenditures justify why falls suffered by elderly people must be considered a public health issue.

The main measure to reduce these falls' occurrence is preventive: adjusting the elderly environment, removing carpets and excessive furniture, and any other source of elderly mobility complication. Physical activity also matters to elderly health maintenance, reducing their fragility (MAZO et al., 2007). Nevertheless, when a fall occurs, the most important goal is to reduce the "time to help". Research identified that the risk for fall sequels are related to the time the victim waits for the assistance offering (TINETTI et al., 1988).

There are many reports of elderly people who, living alone, fell at home and waited hours or even days for proper help. Such situations lead to serious sequels and, in worst cases, to death (YUAN et al., 2015). On the other hand, when the victim receives relief immediately after the fall, its consequences will be as small as possible. Some families opt for personal caregivers, allowing 24-hour monitoring every day. However, due to the expenses of such solutions, most families have to find another one, requiring great patience and commitment to the elder member's health. Elderly people who are not so well supported by family must face the fall risks, since the family may be considered the main source for support and help (WHO, 2007).

In order to minimize the "help response time" and fall consequences, several devices have been developed to enable family notification in elderly emergency situations. Since devices

like these must be usable by people with mental disabilities, and considering that after a fall the victim may be unable to press a button or do anything at all, automatic fall detectors have become relevant and useful, offering confidence to elderly people (IGUAL et al., 2013). The idea of a low-cost solution with high quality, which means greater accuracy, motivates the development of this work. This solution could be used to improve the quality of life of many elderly people, being a good example of how technology may be used for patient-centered care.

The fall detection is normally done through many different technologies (KHAN; HOEY, 2016). The most common one is to acquire motion information using inertial sensors (e.g. accelerometer), allowing the application of different algorithms able to recognize fall events. For this motion acquisition, wearable devices located on the elderly's chest, neck, waist and other body parts may be used. However, for devices located at wrist, the sensitivity and specificity[1] are decreased as consequence of its high complexity motion modeling (NOURY et al., 2008).

Considering the high popularity of watches as wearable devices, which would facilitate its application and acceptance by elderly users, this work proposes the development and evaluation of a fall detector based on inertial sensors located at the user's wrist and presenting high accuracy. According to Yuan et al. (2015), using IMU (Inertial Measurement Unit) devices at the patient's center of gravity is the most reliable choice for spatial orientation, but also the least comfortable. Furthermore, wrist-wearable devices seem to remove the stigma associated to the use of medical or health care devices, as well as present a higher acceptance for being worn at night or during bathing.

The solution proposed in this work may be futurely implemented into an embedded system, allowing its application as a commercial or research device. Although this objective limitates solutions, it is relevant for the goal of helping the lives of the elderly with a low cost and high reliability.

## 1.1 BACKGROUND

The occurrence of falls suffered by elderly people should not be considered a recent or local problem. Its background and consequences are well-known among many families with elderly people. However, a more adequate awareness about the problem could be raised, since

[1] Sensitivity and specificity are terms associated to the classification quality of an algorithm. Sensitivity is related to the classification of a true event as true, while specificity is related to the classification of a false event as false (FAWCETT, 2006). In this work, sensitivity will be directly related to the identification of fall events among different non-fall activities, and specificity will be directly related to avoid the generation of false alarms, suggesting fall events when only non-fall activities are occurring.

a first fall may initiate a series of new falls based on the recurrence factor (ASCHKENASY; ROTHENHAUS, 2006). Also, it affects many people around the world, not allowing a distinction between different countries: it is a global problem.

Solutions for elderly fall detection may be seen since the 1990's (NOURY et al., 2008). They use different techniques to achieve the same objective: automatic fall detection with high accuracy. Solutions based on IMU devices seems to be more popular. Digital image processing is also very applied, but allows only indoor solutions. Researches based on other sensors and techniques are also seen, and may present as interesting results as IMU-based solutions (CHACCOUR et al., 2016).

As a consequence for the high number of different solutions for fall detection under research, different review papers are also available, separating these solutions into categories. For example, Khan e Hoey (2016) evaluates many different works according to the data availability during algorithm tests and validation. On the other hand, Mubashir et al. (2013) classifies different fall detection options into wearable, ambient (audio/video) and vision-based solutions.

In order to be considered an optimal elderly fall detector, some challenges must be overcome. About the technical challenges, a proper solution must have a perfect sensitivity, detecting every fall suffered by an elder person. Also, a high specificity is equally important, since false alarms may generate stress and discomfort, reducing the solution's reliability (NOURY et al., 2008). Another important challenge is that an optimal solution must detect fall events automatically, without any user interference. This is relevant, since after a fall, many elderly people experience fainting or loss of consciousness. An automatic, easy-to-use solution could also be used by patients suffering from dementia-related diseases (CONCEPCION et al., 2016).

About the commercial challenges, in order to be available for a large number of users, the solution must present a low cost and be easy to use without any professional interference. Also, the availability for indoor and outdoor use must be seen as a relevant feature, increasing its applicability. For commercial purposes, some requirements are hard to be properly defined. For example, an optimal solution must be discrete and comfortable, but these aspects depend much more on user expectations than any technical definition. The battery life is also an important topic: long life battery requires less charging cycles, which means less time out of monitoring. (BENNETT et al., 2016).

From a legal point of view, solutions based on monitoring the environment (e.g. audio and video) may be considered offensive to privacy (MUBASHIR et al., 2013). Electromagnetic-emitting solutions located at the chest may offer risks to pacemaker users, requiring a proper evaluation for this application (HAYES et al., 1997). Risks related to bad usage must also

be avoided: using the device wrongly may not offer any risk to the user. For these reasons, legal aspects are relevant to be observed when fall detection solutions are being studied and developed.

This work considers an IMU-based solution located at wrist as an optimal option to overcome the legal and commercial challenges. A wearable device as a smartwatch could be easily used and may attend to all legal requirements. However, the number of solutions under research for this kind of wearable device (wrist-located) is too low. Since the technical challenges to achieve great accuracy with this approach are too hard as identified by Bagnasco et al. (2011), only a small portion of the solutions presented in literature are based on wrist-located wearable devices (BENNETT et al., 2016).

## 1.2 PROBLEM DEFINITION

A well-known definition for falls was presented by the Kellog International working group: ”a fall is an inadvertently coming to rest on the ground, floor or other lower level, excluding intentional change in position to rest in furniture, wall or other objects” (CHACCOUR et al., 2016). Thus, a fall detector must distinguish fall events from ADLs (activities of daily life). Considering a fall event as a critical situation, any algorithm for fall detection must be set to perform the best specificity available for a perfect sensitivity.

As an example, we can consider two algorithms for fall detection: algorithm A presents 100% of sensitivity and 70% of specificity, and algorithm B presents 70% of sensitivity and 100% of specificity. In a scenario where both algorithms were applied to the same learning and testing set, with 50% of samples for fall events and 50% of samples for non-fall events, the accuracy for both algorithms would be the same. However, for this application, algorithm A could be considered more efficient, since sensitivity seems to be a more relevant variable than specificity.

Solutions based on motion-sensing are normally developed using an inertial measurement unit. IMUs may be defined as the combination of two or more sensors able to detect and measure a bodily movement. Typically, an IMU is comprised of an accelerometer and a gyroscope, but it also may present other sensors, such as a magnetometer and a barometer. An accelerometer allows the measurement of translation movements. A gyroscope, on the other hand, allows the measurement of rotation movements. Together, they allow an estimation of a body’s space orientation.

Using an IMU attached to the body of an elderly person, it is possible to measure

the displacement and rotation of the exact point where the IMU is attached. Considering a solution located at the wrist, all the IMU information needs to be processed, in order to translate accelerations and angular rate to spatial orientation and displacement changes. From this new information, patterns of fall events could be identified between many movement acquisitions, leading to a robust solution for the problem.

However, a human wrist is able to perform translation and rotation movements in all the three coordinate axes, even for ADLs. Thus, a proper calculation of the spatial orientation of such a device becomes a complex work, since ADLs and fall events are not always easily distinguished. The chest and the waist, for example, present a much simpler spatial orientation model, but a collar or a belt seems to be less comfortable and discrete than a simple wrist-located device (YUAN et al., 2015). A waterproof *smartband* fall detector could be used 24h a day, allowing uninterrupted monitoring.

The development of an algorithm for a wrist-located wearable device that presents a sensitivity of 100% and specificity equal or higher than 95% for fall detection is the problem this work intends to solve. The evaluation of such an algorithm must also be observed, identifying its reliability.

## 1.3 OBJECTIVES

The objectives of this work can be divided between general and specific objectives.

### 1.3.1 GENERAL OBJECTIVES

The general objective of this work is the development of a reliable algorithm for a wrist-located fall detector based on IMU technology.

This objective is defined by the problem defined previously, which affects many elderly people around the world.

### 1.3.2 SPECIFIC OBJECTIVES

The specific objectives of this work are:

- Understand and estimate the behavior of elderly people wrist movements and spatial orientation using an IMU device;
- Prepare a database composed of fall and non-fall signals acquired using an IMU device;

- Identify which IMU variables have more influence on different fall detection algorithms;
- Evaluate the relevance of a movement decomposition between vertical and non-vertical components for increasing fall detection accuracy;
- Develop two fall detection threshold-based methods (with and without magnetometer data), evaluating their accuracy through the acquired database;
- Compare these methods to other traditional pattern-recognition methods presented on literature, confronting the results presented by each of them;
- Define the best algorithm suggested as a solution for elderly fall detection based on a wrist-located wearable device, justifying such a choice.

## 1.4 WORK CONTRIBUTIONS

The solution developed in this work cannot be confused with a general fall detector. Instead, a fall detector for elderly people considers ADLs as walking, sitting on a chair, reading a book, etc. General fall detectors should care about many other activities as jumping, running, doing sports, etc. In this case, the algorithm complexity might increase too much, and since elderly people are commonly related to low mobility, this complexity growth would not be justified.

Although the solution proposed at this work could be embedded on a wearable device, this implementation will not be discussed here. Also, the tests will be performed on saved data, and not on real time. The focus is to develop and evaluate a proper solution that can be embedded on a wearable device, but its execution may be done in a future work.

Considering the few works presented on literature for fall detection wrist-located solutions, the main contribution of this work is the evaluation of different fall detection methods, based on threshold and machine learning algorithms, defining what is the best approach to solve the elderly fall detection problem considering a wrist-worn device.

## 1.5 SCOPE

This work is presented in three main chapters.

The first chapter is related to the theoretical fundamental of this work. The proper definition of the elderly fall problem, fall detection solutions presented by the literature and

main IMU-based fall detectors are all explained in this chapter. Furthermore, the theory details about employed methods are also presented there.

The second chapter explains the methods approached in this work. Details about the acquisition data system and evaluation protocol are also presented there.

After that, the third chapter presents all the main results for the different approached methods of this work. Also, a discussion about the results is presented, comparing the best achievements and defining the best approach to solve the fall detection problem.

A final chapter concludes the work, highlighting its contribution to the literature, and also presenting the future activities expected to be accomplished.

# 2 THEORETICAL FUNDAMENTALS

In this chapter, the theoretical base for the main concepts and methods presented in this work are discussed. To facilitate its understanding, it is divided into five topics.

The first discusses the elderly falls. Its definition, causes and consequences are well explained, according to the literature. In a second topic, a review of different fall detection solutions are presented. These solutions use IMU variables (e.g. acceleration) and other variables (e.g. sound), presenting different advantages and disadvantages. The third topic compares different IMU-based solutions. The accuracy for each one is reviewed according to the place of the body it must be attached to. A fourth topic brings a mathematical discussion about translation and rotation movements. The quaternions, a mathematical representation used in this work, are also explained. Finally, a last topic presents a theoretical explanation of the methods approached in this work.

## 2.1 FALLS IN THE ELDERLY

The event of an involuntary movement that leads a person to rest in the floor, ground or any other level may be considered a satisfactory definition for a fall. However, it is important to emphasize intentional movements for resting in furniture or other objects as non-fall events (CHACCOUR et al., 2016). The involuntary characteristic of a fall complicates its study, since a voluntary movement simulating a fall will hardly provide the exactly movement details of a real fall. Also, different causes for falls lead to different fall events. A person who falls due to fainting will not react with arms and legs, damping the physical impact. On the other hand, a child who is running and falls may use different movement resources to avoid major consequences.

For these reasons, in order to understand and provide a relevant algorithm to fall detection, the study of fall causes becomes a fundamental topic, allowing the development of a robust solution for all situations. Actually, the best solution for elderly falls would be a preventive approach. Even in elderly care institutions, where many caregivers and nurses are present,

preventive measures must be adopted as a fundamental resource for fall avoidance (FERREIRA; YOSHITOME, 2010). According to Al-Aama (2011), there are many options for fall prevention, as follows:

- Controlled vitamin D supplementation;
- Practice of exercises (e.g. physiotherapy);
- Gradual reduction of psychotropic medication;
- Help and assessment for elderly people who have vision problems;
- Evaluation of cardiac patients, who may need cardiac pacing;
- Environment intervention, making home a safer place to move and stand.

About the practice of exercises, Mazo et al. (2007) also identified that a high level of physical activity is efficient to reduce the risk of fall events, since it increases muscular strength, flexibility and motor control. However, even in an ideal situation where all the preventive measures are taken, the occurrence of fall events is still possible. The purpose of this work is not to remove the necessity of preventive measures. On the contrary, a fall detection system must increase the user's safety, reducing the consequences for a fall, but not avoiding it.

There are many causes for a fall, but they are normally related to the loss of balance. For this reason, the vestibulopathy seems to be extremely associated to a high fall incidence, leading to more complicated consequences than the vestibulopathy by itself (GANANÇA et al., 2006). Also, the fall is considered the most dangerous consequence for the loss of balance and motion difficulty (RUWER et al., 2005).

In order to identify the most relevant causes for elderly falls, Lopes et al. (2007) interviewed 20 women, predominantly aged between 60 and 70 years old. The most frequent cause of falling was related to slips occurred in wet floors. However, it was also reported the occurrence of falls in the backyard, after stumbling on stones. These reports present two important facts about elderly falls. Firstly, a home seems to be the most probable place for falls occurrence. Once the only place where elderly people are normally alone is at home, the most common reported falls with severe consequences are normally observed there. The second fact is related to outdoor occurrence of falls. Home backyards may present a dangerous environment for elderly people, with irregular ground and obstacles (e.g. stones, foliage). Thus, a fall detection system which is not restricted to a fixed environment may be easily adapted to outdoor situations.

Similarly, Guimarães e Farinatti (2005) selected 30 subjects between 72 previously interviewed elderly people. From them, aspects about elderly falls were investigated, highlighting three main possible causes: vision conditions, use of medications and number of associated diseases. About vision conditions, the occurrence of falls among people with ills related to vision were considerably greater than vision healthy people. About the use of medications, a relationship between it and fall occurrence was not well observed. Only when considering elderly people who received 5 or more medications was a correlation between falls and medicament consumption perceived. Finally, the number of diseases was not identified as a relevant aspect for increasing the fall occurrence risk. It seems to be more related individually, suggesting a specific evaluation about how each disease may increase the fall risk when combined to additional variables.

Considering any physical or physiological disorder as relevant for increasing the risk for fall events, hospitals would be a very probable place for elderly patient falls occurrence. And this is confirmed by the work of Abreu et al. (2015), where a statistical analysis of the data acquired from three different hospitals in Cuiabá (Mato Grosso, Brazil) presented a fall incidence rate of 12.6 falls per 1000 patients/day. For this reason, solutions for elderly fall detection are also relevant for a hospital environment, where nurses and doctors could offer immediate help after such event.

A work presented by Tinetti et al. (1988) identified a strong recurrence among elderly fall victims, where approximately 65% of them suffers a new fall in six months. This may be justified by the fear of a new fall as consequence of a first fall. Young e Mark Williams (2015) studied the different elderly state relationship with the fall incidence. According to them, physiological conditions (e.g. reduction of balance control in elderly people) are not the only consequence for increasing fall risks; psychological ones are important as well. The difficulty to allocate attentional resources when different tasks are being performed at the same time may directly increase the risk for a fall event. For this reason, since the fear of falling may affect elderly people's attentional processes, the fall risk is increased as a result.

A fall may be divided into four different phases (NOURY et al., 2008). Figure 1 presents a diagram, where each phase is represented on time (horizontal axis) and height above the ground level (vertical axis).

The first phase is called the pre-fall. In it, the elderly person is performing any normal activity of their daily life, which must be detected as a non-fall event by any accurate fall detection system. The second phase is the critical phase. It may be considered the exact moment when the fall happens, leading the victim's body to the ground, floor or any other lower level.

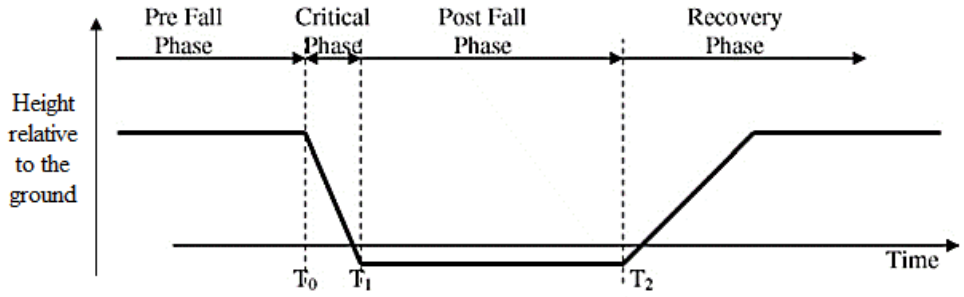


**Figure 1: Diagram representing the four phases of a fall. The horizontal axis represents the time, while the vertical axis represents the body's height related to the ground. Each one of these fall phases can be differently explored by a fall detection algorithm.**

**Source: Adapted from (NOURY et al., 2008).**

Also, this phase has the shortest duration: about 300 to 500 milliseconds. The third phase is called the post fall. It is defined by the time waited by the victims to receive support, or to get recovered by themselves, after a fall event (critical phase). In order to reduce fall sequels, the duration of this phase must be shortened. Finally, the recovery phase is related to movement (intentional or not) to get back to the normal body position.

These four fall phases may be related to the four fall acceleration steps presented by Pierleoni et al. (2015), which is showed in Figure 2. The pre-fall phase is observed as everything before the fall start step. The critical phase is composed by both start and impact steps. During fall start step, the norm of the acceleration vector tends to zero. An ideal free fall would be identified as $0m/s^2$ in all acceleration axis; however, due to the body's reaction and partial absorption (e.g. bending the knees), a human fall is different than a free fall. The impact step will be different for every fall, but magnitude values greater than 2G (approximately $19.6m/s^2$) are normally expected. Aftermath and posture steps are equivalent to the previously mentioned post fall phase. The aftermath step corresponds to a short while when the body is motionless, right after a fall. The posture step is related to abnormal position assumed by the body after a fall, until return to the original position.

These different fall steps or phases propose a relevant discussion, in order to define what will be exactly identified by a fall detection system. For example, wearable solutions located at waist or chest allows an easier detection of post fall phase, which is almost impossible to detect for wrist located devices. However, the impact acceleration magnitude may be higher at wrist located devices, since arms are normally used in a reaction movement to damp a human fall.

The consequences for elderly falls are diverse, depending on the original victim's

health situation, fall severity and help response time. Also, they may be physiological and psychological, leading to the occurrence of new falls, as previously explained.

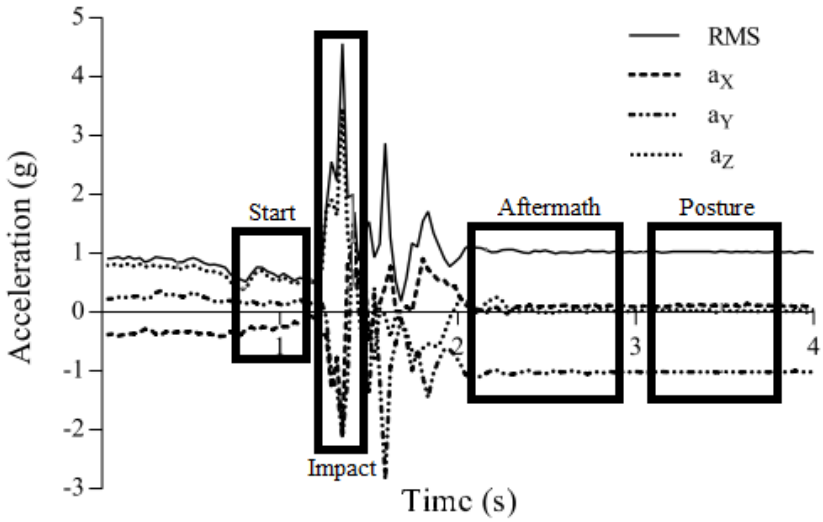


**Figure 2: The four different acceleration steps of a fall. The start step separates a normal activity situation from a fall impact moment (impact step). The aftermath corresponds to a short while when the body is motionless, right after a fall. The posture step is related to abnormal position assumed by the body after a fall, until return to the original position.**

**Source: Adapted from (PIERLEONI et al., 2015).**

From a physiological point of view, bone fractures, muscular traumas and mobility reduction are commonly seen as elderly fall consequences. They are treated, when possible, with hospitalization, medication and physiotherapy (ASCHKENASY; ROTHENHAUS, 2006). On the other hand, although psychological consequences are not so present in literature, they are also relevant. According to WHO (2007), there are several possible post fall sequels (e.g. dependence, loss of autonomy for activities of daily life, confusion, depression, loss of mobility) which reduce the elderly life quality. Also, they are normally related to consequences on friends and family's routine, which may stress the elderly victim even more.

For these consequences, elderly falls must be faced as an extremely relevant public problem. Furthermore, according to Ruwer et al. (2005), they are responsible for 70% of accidental deaths in people aged 75 and over. This is a threateningly high number that could be sharply reduced with the application of the preventive measures previously presented in this work, added to the use of a fall detection system.

An old study performed by Gurley et al. (1996) presents a relationship between fall consequences and the time the victim waits to receive proper relief. According to it, immediate help seems to be crucial. When no help is presented within one hour, the risk of death increases

from 8% to 40%.

After a fall, many elderly people are not able to recover by themselves. As a consequence, they stay on the floor until external help arrives, which can take hours or even days. This situation leads to other non-fall related problems, as hypothermia, dehydration and low blood pressure, increasing the risk for more severe sequels (IGUAL et al., 2013).

About the public spending related to elderly falls, the numbers are also alarming. In Brazil, it is estimated that more than R$160 million (US$48.4 million) were spent by the *Sistema Único de Saúde* - SUS (public health system) in 2015 with bone fracture treatments of elderly people related to fall events (DATASUS, 2015). And the worst: this number is almost twice the estimated for six years before (BALDONI; PEREIRA, 2011). Furthermore, considering the elderly population is about to increase, the public spending related to elderly falls may increase as well. Therefore, solutions able to reduce fall consequences are expected to be even more welcome soon.

## 2.2 GENERAL FALL DETECTION SOLUTIONS

Elderly fall detection systems have been discussed by many authors, with different approaches to reach relevant results. Once many solutions are already available, there are also many reviews presented in literature. These reviews allow a fast comprehension of how technology could be used to change, improve and even save elderly lives.

The number of solutions for elderly fall detection are considerably high, so Boulton et al. (2016) proposed a taxonomy for fall detection systems. As a result, a website is available to any researcher who desires to insert one or more works related to the theme at a FARSEEING (collaborative European Commission) database, using the proposed taxonomy. This idea may be considered relevant to organize and evaluate different solutions properly.

Noury et al. (2008) reviewed some solutions for fall detectors, proposing an approach to classify and evaluate them. In their work, an appropriate terminology is presented. Some important definitions allow a proper identification of different fall detection methods, as follows:

- Accelerometric: detection of specific movements and physical shocks of human body;
- Statimetric: considers the human body's height above ground level to fall detection method;
- Topometric: uses the human body's spatial position to detect falls;

- Eidolimetric: detection using video monitoring of the human body;
- Pheripheral: detection related to behavioral/contextual variables.

This terminology is not concerned with the technology applied on fall detectors. Instead, only information about a fall event is relevant to the method considered. For this reason, it seems to be relevant to distinguish solutions with similar technologies, but different approaches. The solution presented in this work is totally accelerometric, which is normal considering the application of an IMU device located at a human wrist.

Still on Noury et al. (2008) work, the sensitivity and specificity are strongly recommended criteria to evaluate fall detector response. However, as different solutions presented in literature do not use the same testing procedure, a proper comparison between them becomes hard to be accomplished. Nevertheless, it was possible to observe that most part of commercial solutions are worn on the wrist or on a belt even that their performances are considered far from the ideal.

Perry et al. (2009), differently, proposed a review comparing the employment of accelerometers, identifying solutions which use accelerometers as the only source of information, solutions where accelerometer information is combined with other sensors' data and, finally, solutions where no accelerometer is employed. The work concludes that acceleration data is extremely relevant to increase the accuracy of fall detection systems, reducing the false alarm rate.

Mubashir et al. (2013) presented a more expanded evaluation. In their work, the fall detection solutions are divided into three different groups.

The first group is related to wearable device solutions. In this case, the cost efficiency, easy installation setup processes and simple usage requirements evidence wearable devices as user friendly, allowing a large application. However, the necessity for being connected all the time to the user becomes a very intrusive and dependent solution, reducing its reliability.

The second group may be defined as the application of audio and visual data into fall detection methods. Most solutions from this group make use of ambient pressure to detect abnormal events, which is a non-intrusive and cost-effective solution. However, false alarms are commonly seen in these cases, leading to a low detection accuracy.

Finally, the third group is related to image processing solutions. These solutions are becoming more and more common in literature, achieving high accuracy rates. Also, very different methods may be seen for solutions using this approach. But, although cameras are not

considered as invasive solutions, they introduce some ethical issues related to elderly people's confidentiality and privacy. Furthermore, they can be applied only as indoor solutions, reducing the field for its application.

Igual et al. (2013) simplifies this classification into two categories: context-aware systems and wearable devices. Context-aware systems are based on solutions deployed at the environment where the elderly person is located. They are limited to this environment, but the user does not need to care about using or wearing any device. On the other hand, wearable devices are very common and allow great sensitivity, but depending on where they are worn, a high false alarm rate is frequently observed.

Still, their work presents an evaluation of fall detection system trends and challenges. According to them, vision-based, smartphone and machine learning (related to accelerometer data) solutions are expected to be seen more frequently in literature since then. However, elderly acceptance, usability and systems' performance under real condition appear as the greatest challenges to be overcome by these solutions.

Pannurat et al. (2014) also reviewed many fall detection solutions. Related to wearable devices, they presented an evaluation separating the methods by where they can be located. The results presented that the chest is normally selected as an optimal place, but not the most comfortable. Unfortunately, wrist is commonly related to the worst accuracy results.

A different analysis was presented by Khan e Hoey (2016). According to them and considering fall events as rare and unexpected, it is complicated to acquire enough data amount to properly train fall detection solution methods. So, they proposed an analysis according to the data availability to system training and evaluation. Furthermore, machine learning solutions are suggested to be investigated more thoroughly, relying on the fact of low fall data availability.

Studying the different approaches for fall-related system reviews, Chaccour et al. (2016) presented a more complete classification, presented on Figure 3. Firstly, the solutions may be divided between fall detection (FD) and fall prevention (FP) systems. Then, they must be separated into three groups: wearable, non-wearable and fusion systems. This last one may be defined by the combination of wearable and non-wearable devices in a same system.

This approach seems to be more complete, since fall detection and fall prevention are both considered. Besides, some previously cited classification approaches may be also defined inside this model. In the diagram presented on Figure 3, the solution presented in this work may be inserted in the body wear (BW) group, at the bottom left corner.

About commercial application of elderly fall detection systems, Bennett et al. (2016)

highlight the relevance of wearable solutions with a Cisco prediction: wearable devices will increase from 22 million in 2013 to 177 million in 2018. They also consider two main aspects for fall detectors: accuracy and speed. The first is related to reliability of a system and the second to the possibility of association with a protective device, preventing injuries due to falls (e.g. air bags attached to the elder person's hip).

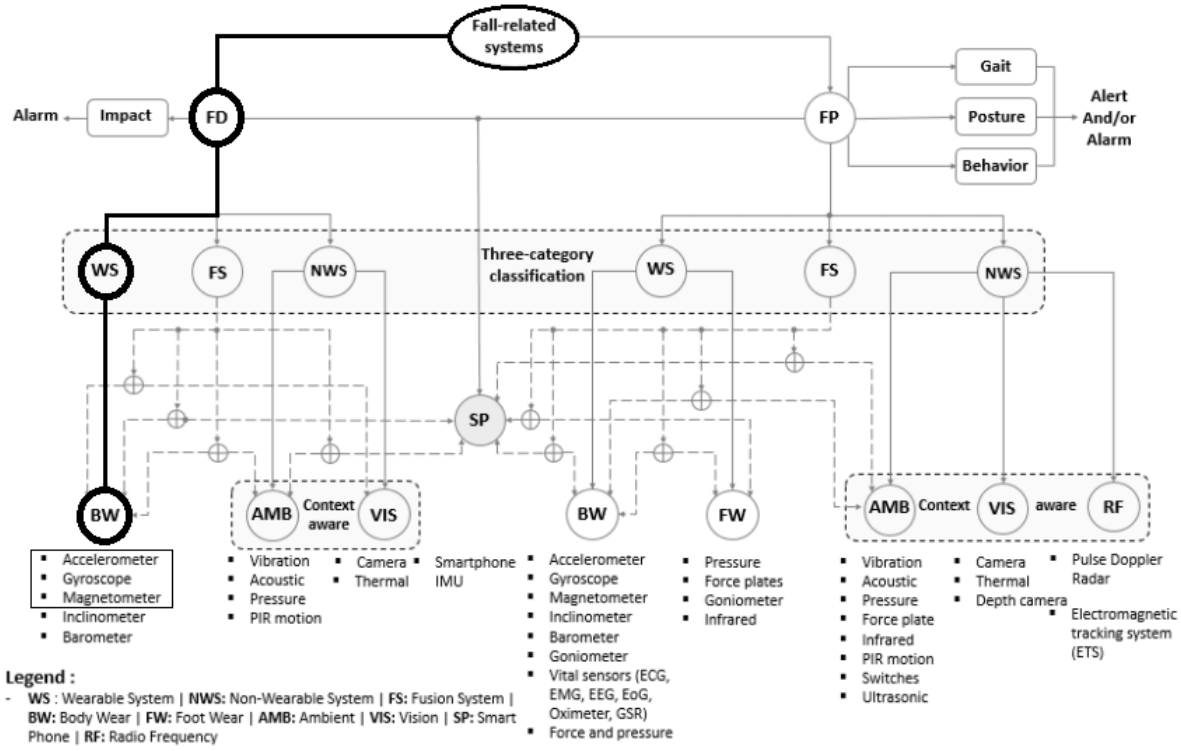


**Figure 3: A fall solution classification. Fall detection (FD) and fall prevention (FP) systems are both considered at this approach. The proposed solution in this work is highlighted: FD (fall detection method instead of fall prevention), WS (wearable system approached) and BW (body wear solution), using accelerometer, gyroscope and magnetometer sensors.**

**Source: Adapted from (CHACCOUR et al., 2016).**

Although IMU-based solution seems to be the most popular options for elderly fall detection systems, different and uncommon technologies also present interesting and relevant results.

Miao Yu et al. (2013) presented a computer vision-based fall detection system. Using a single camera covering a full room environment view, a video of an elderly person was able to be acquired. Later, an algorithm identified the individual silhouettes, detecting abnormal events. Testing the method with twelve people (eight males and four females), a true positive rate of 100% was achieved for a false negative rate of only 3%.

Similarly, using a Microsoft Kinect camera, Stone e Skubic (2015) presented a vision-

based solution. Based on two stages of detection (stand up and lying on the floor), the method was evaluated using a combined nine years of continuously acquired data. For this, the system was installed in 13 apartments, allowing the acquisition of 454 falls, where 445 were performed by simulation and nine naturally occurred by accident. The system achieved (cross validation) 98%, 70% and 71% of detection rate for standing, sitting and lying down falls, respectively, with one false alarm per month rate. However, considering falls that happened when the camera's position was far or partially occluded, this detection rate was considerably decreased.

Using vision-based solutions with a different approach, Ozcan et al. (2013) and Ozcan et al. (2016) proposed solutions based on wearable cameras. Both works are based on two stages: detection of an abnormal event and identification if such event is a fall. However, the second uses more techniques than the first, leading to better results: while the first one presented a detection rate of 87.84%, the second one achieved 93.78% and 89.8% for indoor and outdoor fall detection, respectively.

The complex challenge of an ideal fall detection system extends the possibility of technologies that can be applied. Garripoli et al. (2015), for example, proposed an embedded telehealth system, comprised of a radar sensor and a base station, which is able to detect falls in a real-time monitoring environment. In an indoor and well controlled ambient (which could still be considered limited for commercial applications) it was possible to achieve 100% of fall detection rate, with no false alarms.

Closer to a commercial purpose, Cheffena (2016) proposed a solution based in the audio acquired by a smartphone. In their work, four different machine learning classifiers were evaluated to distinguish fall and non-fall events using only audio information. Although the solution presented some limitations, an accuracy of 98.72% was achieved in the best configuration for the evaluated data.

However, one of the most unusual solutions may be considered the one presented by Daher et al. (2016). Using smart tiles on the floor, they proposed a solution able to detect falls using the force applied to the tiles as information source. The solution was able also to identify different human postures (e.g. walking, sitting), but the presented accuracy is not better than some previous cited works. For example, the fall detection rate is 94.1%, which could be explained by the small amount of data available on learning and testing algorithm steps.

## 2.3 IMU-BASED FALL DETECTORS

An inertial measurement unit comprises one or more sensors related to position and motion information. Combining multiple sensors into a single measurement unit may be efficient to increase information reliability, allowing the development of smart solutions. Allied to this, IMU devices are normally cheap and easy to embed into more complete hardware solutions. Thus, IMU-based fall detectors may be considered the most popular in literature.

Degen et al. (2003) presented a solution based on an accelerometer located at the user's wrist. From acceleration data, three new parameters were calculated, which are more related to the device's velocity than acceleration. Then, three fall phases were attempted to be identified: high velocity towards the ground, impact and posterior inactivity. The algorithm presented success in forward fall detection, with a rate of 100%. However, for backward and sideways falls, the detection rate was lower than 60%.

Although the results presented in their work were far from ideal, the concept of using velocity to detect falls was also defended by different research. Wu (2000), using cameras and visual markers for example, identified similar horizontal and vertical velocity magnitudes on different human body fall movements. This behaviour distinguish from most part of ADL acquired information.

Fall detection methods based on acceleration thresholds are very common, due to the expected physical impact related to falls. Kangas et al. (2007) evaluated different approaches for threshold setup on fall detection solutions related to accelerometer based method. The tests were performed considering the best specificity for an ideal sensitivity (100%), in three different body places: waist, head and wrist. Evaluating the solution with data acquired from two subjects who performed fall and ADL activities, it was possible to achieve 100% of accuracy for the solution located at head, but only 75% at wrist.

With a similar solution, Bourke et al. (2007) evaluated a threshold-based algorithm using triaxial accelerometer data located at the user's thigh and trunk. In their work, two different thresholds were evaluated: the minimum and maximum value during the acceleration peaks. Configuring the system for 100% of sensitivity and testing it with 240 fall and 240 non-fall acquired activities, it was possible to achieve 100% and 83.33% of specificity for the solution located at the trunk and the thigh, respectively. In both cases, applying the threshold on the maximum values presented significantly better results than applying it to the minimum values of the acceleration peaks.

Many commercial IMU devices presents additional sensors than the three previously

mentioned. A good example is barometric sensors, commonly used as altimeters in wearable applications. In the work presented by Bianchi et al. (2010), barometric information was combined with triaxial accelerometer data, allowing a more complex fall detection method. To develop a proper evaluation of barometric data relevance, three different algorithms were tested. The first was based only in acceleration threshold methods, which allows a physical impact detection. The second algorithm tries to evaluate the final posture along with the first one. Finally, the third one makes use of barometric data in order to identify altitude changes. Acquiring data from 20 volunteers wearing the device at the waist, the achieved accuracy for the three algorithms were 70%, 85.3% and 96.9%, respectively. This confirmed the relevance of an additional information source (e.g. barometric sensor) to increase system accuracy.

Trying to develop a simpler algorithm, Bagnasco et al. (2011) proposed an accelerometer-based solution where a free fall was attempted to be detected. During a perfect free fall, acceleration is zero for the three-measurement axis. As the fall suffered by an elderly person is very different than a perfect free fall, different thresholds were tested, placing the device at subject's waist, chest and wrist. Although many accelerometers allow an easy configuration for free fall detection (even setting digital output ports automatically), the achieved results were far from the ideal. The best result was achieved for the device in the chest (88% and 100% of sensitivity and specificity, respectively). Considering the device located at the wrist, the best sensitivity and specificity achieved were 71% and 89%, respectively.

Using a machine-learning algorithm based on a cascade-AdaBoost-support vector machine (SVM), Cheng e Jhan (2013) proposed a solution acquiring data from a simple triaxial accelerometer. Tests were performed wearing the device at the left and right ankle, chest and waist. The best accuracy achieved was 98.48%, being the waist and chest identified as the best body locations for wearing the proposed device.

Tong et al. (2013), differently, proposed a method based on a statistical concept called Hidden Markov Model (HMM). Similar to the previously mentioned work, only a triaxial accelerometer was employed, but the tests were performed wearing the device at the upper trunk of the subjects, near the neck. In order to evaluate the method, 80 fall and 40 non-fall signals were acquired from eight volunteers. The method was divided into two different approaches: fall prediction and fall detection. The fall detection approach achieved 100% accuracy, offering a very relevant contribution to literature. The fall prediction approach presented great results as well: 100% sensitivity and 88.75% specificity. The only limitation of their solution is the place where the device must be worn.

In order to develop a system able to detect falls before they happen, Liu e Lockhart

(2014) proposed an algorithm able to identify the pre-fall phase using accelerometer and gyroscope data. The method calculates the human trunk extension angle, trying to perceive a movement towards the floor. Testing the device at the trunk of ten elderly participants (an apparatus to avoid real fall consequences was prepared), the algorithm was set for 100% of sensitivity, allowing to reach 95.65% of specificity. Detecting a fall before it happens may be interesting for the development of solutions to reduce fall impact intensity.

Similarly, Lee et al. (2015) developed two algorithms based on accelerometer data acquisition. The first was based on vertical velocity and the second was based on acceleration magnitude only. The device was placed at the waist of eleven experimental participants. The algorithms were developed for two classifications: fall versus near-fall events and fall versus ADL events. In this case, near-fall events may be defined as movements similar to fall situations, but followed by human position recovery, avoiding the fall. This approach seems interesting to evaluate fall detection solutions specificity. The best result was presented by the first algorithm, reinforcing the velocity relevance on fall detection principles. For a general environment (fall, near-fall and ADL) of fall detection, the solution achieved an accuracy higher than 95%.

Kambhampati et al. (2015), using an accelerometer, developed a method based on cumulants and combined to a hierarchical decision tree classifier. The objective was to identify different characteristics of a fall from acceleration information, against more simple approaches based on only threshold methods. The device was developed to be worn at the waist, and presented an accuracy of 96.91% for the best configuration.

Increasing the complexity of the IMU sensor fusion, Pierleoni et al. (2015) developed a method for fall detection based on the combination of accelerometer, gyroscope and magnetometer. Placing the device at user waist, the system was able to identify different characteristics of a fall event, including pre-fall analysis and aftermath position. The sensor data fusion algorithm applied was the Madgwick's method, a simplification of Kalman-filter[1] Tests were performed with ten volunteers, according to two different protocols involving different fall signals. For the simplest protocol, the system achieved 100% of accuracy, but for the second one, the highest accuracy presented was 90.37%. The second protocol is similar to the first one, but two different fall simulation signals were included: backward falls ending in sitting position and syncope (leaning against a wall and then slipping vertically).

In order to embed a fall detection solution into a commercial product, some different

[1] Kalman-filter is considered in literature as a relevant method for filtering and conditioning different combined sensors data (KOWNACKI, 2011). However, due to its high computational complexity, particularly for embedded systems, different approaches have been developed to achieve similar results requiring less processing resources (PIERLEONI et al., 2015).

questions appear. One of them is about battery lifetime, a characteristic related to the system's power consumption. Taking that into account, Yuan et al. (2015) proposed different algorithms based on accelerometer information, but discarding information of low levels of activity from the device to save the processing time for interesting moments of evaluation. Furthermore, the solution can identify three different ADL patterns: walking, quiet and random. Tests were performed for the device worn at the wrist of four different subjects. The system achieved an accuracy of 94.3%.

Previously, an older work also presented a wrist-worn device, able to detect falls and measure some biomedical signals from the user, such as heart rate, blood pressure and respiration rate (KANG et al., 2006). Although the device size was too big for daily use, it seems to be an interesting solution for health care unit application. Using only a two-axis accelerometer as data source, the system was able to achieve a detection rate of 91.3% (complete accuracy was not informed).

Also using barometric and accelerometer sensors, Wang et al. (2016) presented a low power solution able to work around 664 days (estimated) with 93.0% and 87.3% of sensitivity and specificity, respectively. Their method uses a binary decision tree algorithm and was tested on eleven experimental participants through a prototype similar to a lanyard (to be used on the neck).

Increasing system information, Sabatini et al. (2016) proposed a solution based on accelerometer, gyroscope and barometer data. In their work, the IMU sensors are combined to calculate vertical velocity and height displacement. Then, the barometer is used to acquire altimeter information, allowing the system to increase its height measurement accuracy. Tests were performed by twenty-five subjects wearing the device at the right anterior iliac spine. The testing protocol was extensive, including five and seven different fall and non-fall movements, respectively. The algorithm was able to achieve 100% of accuracy when detecting falls by performing impact and posture analysis.

Pierleoni et al. (2016) also added barometric sensor information to their previous work, increasing the number of movements approached in the testing protocol. The tests were performed by twenty-five volunteers, and the results were compared to other works in literature. The average accuracy achieved was around 99.8%, a high rate even for waist worn solution devices.

Using accelerometer information from a smartphone, Concepcion et al. (2016) tested some differently awarded algorithms for ADL and fall event identification. For the system evaluation, data from 30 volunteers was acquired and combined to data from three different

public datasets. The results presented an average accuracy rate of 95% for the identification of many events: falling, walking, running, stopping, driving, etc.

Valcourt et al. (2016), also using a smartphone as an IMU device but acquiring gyroscope data along with accelerometer information, proposed a two-step algorithm for fall detection. The first step is responsible for identifying where the smartphone is selected: T-shirt chest pocket, waist pocket, etc. This is an interesting approach, since a smartphone may be located at different body places, affecting algorithms detection accuracy. The second step concerns the fall detection algorithm, based on parameters resulting from the first one. The system was tested with six experimental participants, and presented an average accuracy of 81.3%. Although the accuracy rate seems to be low, the evaluation of different smartphone positions brings an interesting point for the discussion of such solutions.

Still on smartphone based solutions, Ando et al. (2016) combined the information from accelerometer and gyroscope from an Android smartphone. In their work, a solution for identification of different ADL and fall events were presented. The algorithm considers that different movement patterns are responsible for specific inertial quantities, related to acceleration and angular velocities. Therefore, by different threshold combined methods, the system can detect forward, backward and lateral falls, up and down stairs, lying down and sitting down. Tests were performed by ten subjects, presenting 81% and 98% of sensitivity and specificity, respectively.

Differently, Pannurat et al. (2017) proposed an algorithm based on a time control mechanism and machine learning using a triaxial accelerometer. The system was tested at different body places: head, arm, chest, waist, wrist, thigh and ankle. So, an extensive analysis about the relationship between sensor position and system detection rate was performed, based on data collected from sixteen experimental participants. For the tests, fourteen and twelve fall and non-fall events were evaluated. The algorithm, able to detect pre-fall, fall impact and aftermath, presented the best accuracy rate for waist worn configuration: 86.54% (only pre-fall analysis), 87.31% (including fall impact detection) and 91.15% (considering aftermath position as well).

About threshold and machine learning algorithms, Aziz et al. (2017) compared both methods using triaxial accelerometer data from a device located at the user's waist. For the evaluation, five different threshold methods and five different machine learning algorithms were tested with the same device under the same environment. Ten young subjects performed more than 200 fall and 200 non-fall movements, allowing the development of a relevant analysis. The best accuracy achieved was 96% for the machine learning algorithm (SVM method) and 94% for the threshold-based algorithm (Kangas3Phase).

Evaluating all these solutions, it is possible to perceive how threshold-based algorithms

are being less studied over time. On the other hand, different methods (e.g. machine learning) appear as new possible solutions for overcoming detection accuracy challenges. Furthermore, few works are related to wrist worn solutions, while waist seems to be the preferred one. This can be explained by the human center of gravity, which is located near the waist (considering a standing position). Therefore, more information about the human body's position is available at the waist than other traditional wearable positions, like chest, wrist or head. Thus, after a fall, a wrist may be spatial oriented in many positions, complicating the possibility for a fall aftermath detection.

Table 1 presents a brief summary of all the described IMU-based fall detection solutions. The results are expressed according to the related accuracy, but the lack of a standard protocol hampers a proper comparison, reducing the information reliability.

**Table 1: Comparison of different IMU-based fall detection solutions. The methods are distinguished by the employed sensors and by the threshold-based (TH) and machine learning (ML) characteristics. The best results are related to the accuracy (AC), sensitivity (SE) and specificity (SP) values presented by the references.**

| Reference | Method | Configuration | Best results |
|---|---|---|---|
| (DEGEN et al., 2003) | Accelerometer - TH | Wrist | AC: 65% |
| (KANG et al., 2006) | Accelerometer - TH | Wrist | SE: 91.3% |
| (KANGAS et al., 2007) | Accelerometer - TH | Waist, head and wrist | Head – AC: 100% |
| (BOURKE et al., 2007) | Accelerometer - TH | Thigh and trunk | Trunk – AC: 100% |
| (BIANCHI et al., 2010) | Acc. and barometer - ML | Waist | AC: 96.9% |
| (BAGNASCO et al., 2011) | Accelerometer - TH | Waist, chest, wrist | Chest – SE:88% SP:100% |
| (CHENG; JHAN, 2013) | Accelerometer - ML | Ankle, chest, waist | Waist – AC: 98.48% |
| (TONG et al., 2013) | Accelerometer - ML | Trunk | AC: 100% |
| (LIU; LOCKHART, 2014) | Acc. and gyroscope - TH | Trunk | SE: 100% SP: 95.65% |
| (LEE et al., 2015) | Acc. and gyroscope - TH | Waist | AC: 95% |
| (KAMBHAMPATI et al., 2015) | Accelerometer - ML | Waist | AC: 96.91% |
| (PIERLEONI et al., 2015) | Acc., gyro. and magnet. - TH | Waist | AC: 90.37% |
| (YUAN et al., 2015) | Accelerometer - ML | Wrist | AC: 94.3% |
| (WANG et al., 2016) | Acc. and barometer - TH | Neck | SE: 93.0% SP: 87.3% |
| (SABATINI et al., 2016) | Acc., gyro. and barom. – TH | Waist | AC: 100% |
| (PIERLEONI et al., 2016) | Acc., gyro, magnet. and barom. – TH | Waist | AC: 99.8% |
| (CONCEPCION et al., 2016) | Accelerometer – TH | Waist | AC: 95% |
| (VALCOURT et al., 2016) | Acc. and gyroscope – TH | Undefined | AC: 81.3% |
| (ANDO et al., 2016) | Acc. and gyroscope – ML | Waist | SE: 81% SP: 98% |
| (PANNURAT et al., 2017) | Accelerometer - ML | Many | Waist - AC: 91,15% |
| (AZIZ et al., 2017) | Accelerometer – TH/ML | Waist | AC: 96% |

## 2.4 MOVEMENTS AND SPACIAL ORIENTATION

In order to understand how an IMU device can be able to identify different human movement patterns, some concepts about analytic geometry must be studied. In this work, two main movement types will be described: translations and rotations. It is important to understand these movement characteristics to define which sensor is more appropriate to measure the intensity of each one (MADGWICK et al., 2011).

A translation movement may be defined as a displacement from one point in space to another one. Considering the inertial characteristic of a body, translation movements are normally related to the force applied to it, leading to a movement over a specific axis. A translation movement may be easily represented by the Cartesian coordinate system. For example, consider the position $t$ of an object defined by (1), where $x$, $y$ and $z$ represent its displacement over the three Cartesian axis, and the unitary displacement is respectively represented by $\hat{i}$, $\hat{j}$ and $\hat{k}$ (UICKER et al., 2003).

$$t(x,y,z) = x\hat{i} + y\hat{j} + z\hat{k}. \tag{1}$$

Then, considering the initial position as $t_0 = t(0,0,0)$ and the final position as $t_1 = t(4,-2,6)$, the translation movement may be represented as $\Delta$T on (2), where $\Delta$T may be defined as (3):

$$t_1 = t_0 + \Delta T, \tag{2}$$

$$\Delta T = 4.\hat{i} - 2.\hat{j} + 6.\hat{k} = t_1 - t_0. \tag{3}$$

Another important characteristic of translation movements are the commutative and associative properties, represented by equations (4) and (5), respectively (UICKER et al., 2003). These characteristics allow an easy representation of combined translation movements:

$$t_0 + t_1 = t_1 + t_0, \tag{4}$$

$$t_0 + (t_1 + t_2) = (t_0 + t_1) + t_2. \tag{5}$$

The accelerometer is the most common IMU sensor for translation movement measurement. As its name suggests, an accelerometer is a device able to measure acceleration in one, two or three dimensions, according to its configuration. A typical triaxial accelerometer, when stopped at a fixed position, will measure a constant value with magnitude of 9.81m/s$^2$ pointing to the center of the earth: the gravity. When measuring the acceleration of a body using an accelerometer, gravity must be considered, since its value will always be present on the measurements.

By the acceleration $a(t)$, velocity $v(t)$ and displacement $d(t)$ on instant $t_f$ can be easily

calculated through a single and double integration over time, respectively represented by (6) and (7) (UICKER et al., 2003):

$$v(t_f) = \int_0^{t_f} a(t)dt, \tag{6}$$

$$d(t_f) = \int_0^{t_f} v(t)dt. \tag{7}$$

Due to noise on acceleration measurement by accelerometers, an error is expected on calculated velocity and displacement, requiring filtering for acceptable values. At this point, the identification of a body could be easily calculated only by accelerometers, since only three degrees of freedom are expected: displacement over x-axis, y-axis and z-axis (UICKER et al., 2003). However, three additional degrees of freedom must be understood and investigated.

A rotation movement may be defined as a spatial orientation change, without displacement. This movement may be represented by the rotation over the three Cartesian axes with origin at the center of object's body, defining the three additional degrees of freedom previously mentioned. Similarly to translation movements, a spatial orientation $r$ may be defined as the combination of three different angles, commonly referred as $\phi$ (also known as *roll*), $\theta$ (also known as *pitch*) and $\psi$ (also known as *yaw*), representing the rotation angle around the x, y and z axes, respectively (PIERLEONI et al., 2016).

Therefore, a final spatial orientation of a body can be defined as the consequence of a rotation movement on its initial position. The accelerometer is also able to estimate a spatial orientation, according to the gravity acceleration components on each axis. However, two problems avoid a correct identification of the body spatial orientation only by accelerometer data: the dynamic state of a body and the gimbal lock (PIERLEONI et al., 2016).

When a body is static, the expected acceleration magnitude from the three axis components of an accelerometer is known: the gravity acceleration. However, when the body is performing a rotation movement, additional acceleration may appear in the three axes, avoiding a proper estimation of the instantaneous orientation. A common solution for this problem concerns the application of a gyroscope as an additional sensor.

A gyroscope is a sensor able to measure the angular velocity of a body in one or more axis. A triaxial gyroscope, for example, will present 0 $degrees/s$ while the sensor is static, which means no relevant information in this situation. However, when the device is rotating, the integration of the angular velocity represents angular changes in *roll*, *pitch* and *yaw* values.

For this reason, while accelerometers are considered relevant sensors for calculating orientation when the system is static, gyroscopes are relevant to measure orientation changes when the system is dynamic.

The combination of accelerometer and gyroscope data may be also called as sensor fusion. Similarly to the accelerometer, due to noise on gyroscope measurements, an integration of its angular velocity will also present an error on the spatial orientation, commonly known as gyroscope drift. Although this sensor fusion appears to be enough to estimate the spatial orientation of a body, the second problem is still unsolved (MADGWICK et al., 2011).

The gimbal lock is a traditional problem for spatial orientation systems based on three axes for rotation measurement. Generically, it defines the undesirable effect of the loss of one degree of freedom as consequence for a specific spatial orientation. An example of how this can happen is presented in Figure 4. In the picture, while the system is under gimbal lock effect, the innermost gimbal is unable to perform a *pitch* rotation movement, unless the gimbal positions are changed.

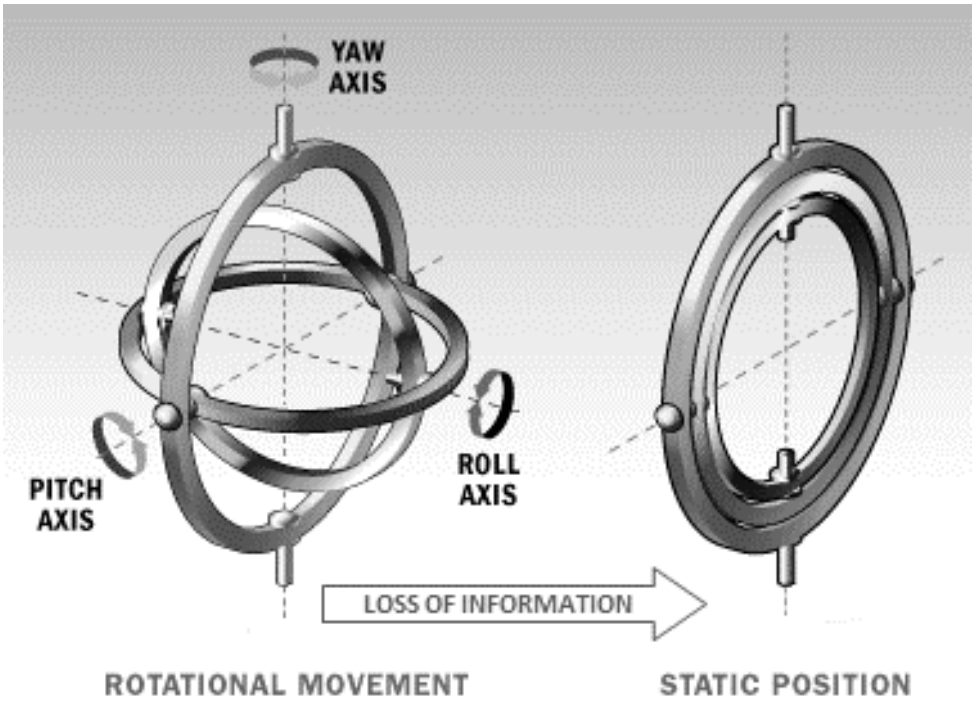


**Figure 4: An example of gimbal lock effect. When the rotation axis are aligned, a system degree of freedom is lost. While the system is under gimbal lock effect, the innermost gimbal is unable to perform a *pitch* rotation movement, unless the gimbal positions are changed.**

**Source: Adapted from (STRICKLAND, 2008).**

Bringing this problem to a fall detection environment, the gimbal lock may be described as the loss of information about a spatial orientation in specific static positions. For

example, consider a static IMU device whose z-axis rotation is perfectly aligned to the gravity axis. In this situation, the accelerometer presents $9.81 m/s^2$ at the z axis, and zero in both x and y axes. Furthermore, the gyroscope presents zero in all three axes, since the device is static, preventing it from being useful. At this moment, there is not enough information for absolute spatial identification of the IMU device.

In other words, related to spatial orientation, there are two conditions for a body: static and dynamic. When the body is under a dynamic condition, the gyroscope is relevant to bring information to the final spatial orientation. However, the original orientation must be known, and it is normally related to a static condition. In this case, the accelerometer may not be enough to calculate the spatial orientation when a gimbal lock occurred. To solve this problem, a magnetometer can be employed (MADGWICK et al., 2011).

A magnetometer may be defined as a sensor able to measure magnetic intensity. Typically, when assembled into IMU devices, magnetometers measure the magnetic intensity components of one or more axis. Inside an environment free of magnetic anomaly, such a sensor will present the magnetic intensity of the earth, and the combination of three axis information will be related to the earth's north magnetic pole.

For this reason, a magnetometer presents an important spatial reference for any IMU device. Furthermore, when the device is in a static condition, magnetometer data can be combined to accelerometer data to escape from gimbal lock ambiguity. Therefore, the combination of the three mentioned sensors on an IMU device allows a highly reliable solution for spatial orientation and displacement.

As expected, the fusion of three different sensors can be a complex task. Also, considering an IMU device located at the wrist, this fusion will require a more complex algorithm than if the IMU device was located at the waist or chest (BENNETT et al., 2016). This can be explained by the comparison of how wrist, waist and chest are normally moving during an ADL performance. A waist will slowly translate in all the axis, but will rotate in only one, normally. Only when a lying down position is assumed, the other rotation axis may be affected. A chest, differently, can perform an additional slow rotation on a second axis (when tying the shoes, for example). However, neither waist or chest moves like a human wrist, which performs quick translation and rotation movements in all three axes. A sensor fusion, in this case, requires a higher sampling rate and a more robust filter (YUAN et al., 2015).

Another point to consider is the system's representation. A traditional Cartesian model may not be able to properly describe the spatial orientation of a moving body. This happens mainly because rotation movements, different than translation movements, do not have commu-

tative and associative properties. For example, considering $R(\phi)$, $R(\theta)$ and $R(\psi)$ as a rotation movement over the axis x, y and z, respectively, then any spatial orientation $S$ may be defined as a sequence of different rotations, as presented in (8) (GOLDSTEIN et al., 2007):

$$S = R(\phi)R(\theta)R(\psi). \tag{8}$$

However, rotation movements do not have commutative and associative properties. So, it is important, for example, to understand the consequence of (9):

$$R(\phi)R(\theta)R(\psi) \neq R(\psi)R(\theta)R(\phi) \neq R(\theta)R(\psi)R(\phi). \tag{9}$$

In other words, the order of the rotations directly affects the final spatial orientation. In order to simplify this approach and facilitate an algorithm development, a different mathematical representation can be applied, called quaternions (MADGWICK et al., 2011). This model is similar to complex numbers, where a spatial orientation $Q$ may be defined by (KUIPERS, 2002):

$$Q(a,b,c,d) = a + bi + cj + dk, \tag{10}$$

where $i^2 = -1$, $j^2 = -1$, $k^2 = -1$, $i.j = k$, $j.k = i$, $k.i = j$, $i.k = -j$, $j.i = -k$ and, finally, $k.j = -i$. Also, the same spatial position may be represented by

$$Q(a,\vec{v}) = a + \vec{v}, \tag{11}$$

where

$$\vec{v} = bi + cj + dk. \tag{12}$$

This mathematical model presents a lot of different properties which are not the focus of this work (e.g. multiplication and inverse quaternion) (KUIPERS, 2002). One of them is the definition of an unit quaternion $q$, which means a quaternion where its magnitude, described by (13), is one:

$$|Q(a,\vec{v})| = \sqrt{a^2 + |\vec{v}|}. \tag{13}$$

Considering $\upsilon$ as the unit vector of $v$, the unit quaternion may be defined by (14), whose proof may be seen in (15):

$$q(\alpha,\upsilon) = Q(\cos\alpha, \vec{\upsilon}.\sin\alpha), \tag{14}$$

$$|q(\alpha,\upsilon)| = \sqrt{\cos\alpha^2 + \vec{\upsilon}^2.\sin\alpha^2} = \sqrt{\cos\alpha^2 + \sin\alpha^2} = 1. \tag{15}$$

Thus, a unit quaternion can be applied to describe a spatial orientation by a rotation of angle $\alpha$ around a unit vector given by $\upsilon$. It simplifies the representation of multiple rotations, as the one described on Equation (9), by a single representation easier to be applied into computing algorithms.

The unit quaternion representation is used by the algorithm developed by Madgwick et al. (2011). By using it, Madgwick's algorithm is able to calculate the three angles related to the device spatial orientation more accurately. So, better results related to movement decomposition are expected to be achieved when Madgwick's algorithm is used instead of only accelerometer and gyroscope based methods.

## 2.5 THEORY BEHIND THE METHODS

Considering the relevance of elderly fall problem, this work proposes the development and evaluation of a fall detection system. Furthermore, as previously shown, few solutions have been developed to be wrist-worn, even regarding the fact that *smartbands* and *smartwatches* are already common and popular wearable devices. The complexity of a fall detection algorithm for a wrist-worn device relies in the high number of movement degrees of freedom related to the wrist position. So, this work presents two main algorithms for fall detection (with and without magnetometer) based on traditional concepts from the literature for threshold analysis, involving acceleration (LEE et al., 2015), velocity (WU, 2000) and displacement (PERRY et al., 2009), whose evaluation is performed by traditional approaches of accuracy estimation and qualitative analysis.

Most of the solutions presented in this work are based on different threshold algorithms combined with event detection time analysis. Since a fall is normally related to a physical shock after a vertical displacement of the human body gravity center, threshold methods are intuitively relevant for such events detection (PIERLEONI et al., 2016). A threshold algorithm may be applied to different variables, directly and indirectly. For example, a threshold related to acceleration peaks will evaluate the data acquired from the accelerometer, while a threshold related to vertical displacement may consider the combined data from different sensors to identify a new variable related to vertical displacement. These possibilities allow different threshold approaches, achieving different results according to the fall characteristics selected to be evaluated (BOURKE et al., 2007).

Combined to a threshold algorithm approach, a time-analysis may be also relevant for a threshold-based algorithm, at least in two different situations. The first is related to the values

integrated over time. Since the data acquired from IMU sensors presents noise from different frequencies (including DC noise), a simple discrete integral would accumulate an error over time, leading to wrong values even for a static device (MADGWICK et al., 2011). For this reason, a window integration may be applied, considering a limited number of previous data into integral calculation. Although this can be considered enough to solve the error accumulation problem, the integration window size becomes an additional variable able to change the algorithm accuracy (QUADROS et al., 2017).

The second time-analysis is related to the combination of different threshold events detected. For example, an algorithm for fall detection could identify the minimum value of acceleration magnitude by a first threshold, followed by the maximum value (peak) of acceleration magnitude detected by a second threshold (SABATINI et al., 2016). However, in order to confirm that both events are related to a same fall, a time evaluation becomes necessary, identifying the time difference between the maximum and minimum peak. This evaluation leads to a variable related to time, which is also responsible to influence algorithm accuracy (QUADROS et al., 2017).

So, although threshold algorithms seem to be more simple to apply to fall detection system, a great number of variables may increase its complexity, requiring extensive tests to define the best configuration for a general scenario. The Figure 5 presents a diagram, where different signals, parameters and thresholds analyses are shown to exemplify how complex an optimal threshold-based algorithm definition may become. This evaluation is also approached in this work, as it will be shown in the next chapters.

Different sensors were employed in this work, according to the fall characteristics expected to be identified in each algorithm. Increasing the number of sensors into the fusion, more information becomes available. For example, the sensors' fusion can allow the body's spatial orientation calculation, making the movement decomposition between vertical and non-vertical components possible. This decomposition may be considered as a relevant factor for increasing detection accuracy in threshold-based algorithms (WU, 2000).

In the work presented by Madgwick et al. (2011), a solution to combine information from an accelerometer, a gyroscope and a magnetometer is developed. For this, quaternions are calculated and, as one of the results, the spatial orientation is estimated. Although the solution is much simpler than a traditional Kalman-based algorithm, the achieved results were similar. The purpose of the algorithm presented by Madgwick was not the development of a fall detector, but its employment in this work offers a reliable solution for the three IMU sensors' fusion (PIERLEONI et al., 2015).

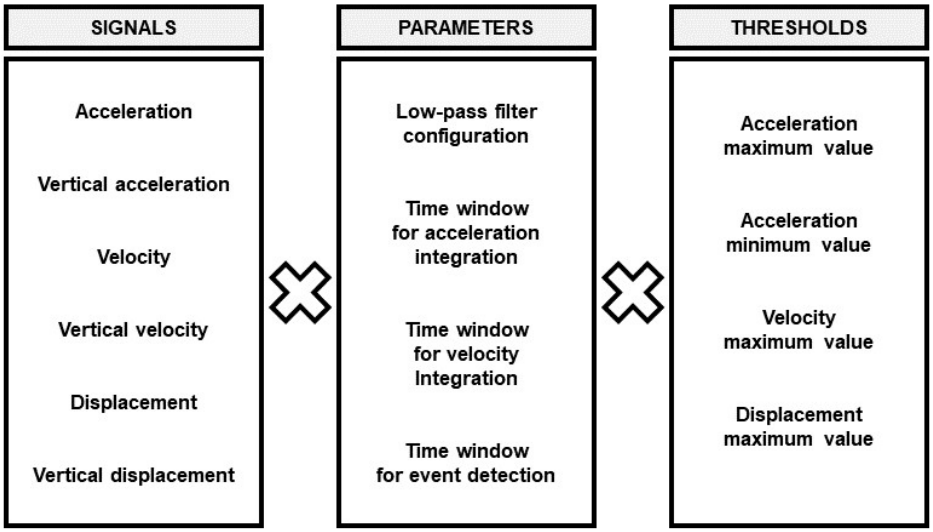


**Figure 5: Diagram about different threshold-based algorithms configuration. A right configuration is responsible for the achievement of better results combining all these variables: different available signals, several algorithm parameters and efficient threshold values.**

**Source: Own authorship.**

Using the spatial orientation resulting from Madgwick's algorithm through the sensors' fusion, the vertical component of the device movement may be calculated, allowing new variables to be evaluated by threshold-based algorithms. Furthermore, some configuration parameters from Madgwick's algorithm can be adjusted in order to achieve the best result for each scenario.

On the other hand, as presented in the solutions' review, machine learning algorithms have become more and more frequent in the literature related to fall detection solutions (TONG et al., 2013; KHAN; HOEY, 2016; YUAN et al., 2015; ANDO et al., 2016). A machine learning approach may be considered extremely relevant, once a threshold-based only algorithm is highly susceptible to false positives, reducing its specificity (AZIZ et al., 2017).

In this work, different machine learning methods were evaluated. These methods are all based on supervised learning, which means that all the class labels are known and previously defined during the algorithm learning (DUIN; PEKALSKA, 2016). Furthermore, different features were evaluated, similarly to the evaluation performed for threshold-based algorithms. Even the spatial orientation resulting from Madgwick's algorithm was considered, in order to check the best accuracy possible for machine learning methods.

There are different machine learning methods present in the literature. In this work, the most traditional options for the problem scenario were selected, allowing a comparison

among their accuracy. Furthermore, by evaluating the machine learning algorithms under the same testing data set applied for threshold based algorithms, a comparison between them becomes possible, allowing a better understanding of such solutions for fall detection systems. These different machine learning algorithms present relevant characteristics for a fall detection environment, so five of them were evaluated in this work, as follows.

The SVM (Support Vector Machine) method is largely found in literature related to fall detection solutions. It was developed based on a machine learning paradigm known as statistical learning. This approach, different than other traditional approaches for classification problems, has been applied in scenarios where the available data amount for system training is limited (BISHOP, 1995). Considering fall occurrence as events complex to be reproduced in large quantity (at least in a short period of time), this approach becomes quite appropriate for a fall detection evaluation, justifying its popularity in the literature, evidenced by many works such as (CHENG; JHAN, 2013) and (AZIZ et al., 2017).

Similarly, logistic regression is also recommended to be used when the amount of available data for the system learning is limited (BISHOP, 1995). Yet, this approach works with the relationship between the proper classification for a data set and the different features evaluated from it, by estimating probabilities and using a cumulative logistic distribution. So this method is also evaluated in this work, offering an approach slightly different than the SVM one, since it presents the classification result in terms of probability.

Another well-known machine learning approach is the LDA (Linear Discriminant Analysis). The objective of this method is to reduce the system to a lower dimensional space, maximizing the separation between classes so its complexity and required processing resource are reduced, as well as to avoid the possibility of overfitting (i.e. a classifier which is, as consequence of a too long optimization, adapted to noise instead of relevant data information) (CHERKASSKY; MULIER, 1998). In this work, this machine learning method may present an interesting solution for low computing cost, facilitating a commercial application of such solution.

The fourth method evaluated is the K-Nearest Neighbors. In this approach, the feature vector classification is performed according to the previous classified feature vectors, associating it to the one which presents the most similar characteristics (closest in terms of Euclidean distance) (BISHOP, 1995). Since the classification is simply based on distances related to a training set, this method may be considered one of the most simple machine learning algorithms.

Finally, the Decision Trees approach can be considered one of the most common

method for fall detection solution present in literature. This can be evidenced by many works previously cited (KAMBHAMPATI et al., 2015; YUAN et al., 2015; AZIZ et al., 2017; WANG et al., 2016; CONCEPCION et al., 2016). Its popularity was one of the reasons why this machine learning method was selected to be evaluated in this work.

In a Decision Tree based machine learning, different binary classifications (if a numeric classification is approached then the correct name is Regression Tree) are performed, related to different variable characteristics (HAYKIN, 1998). These classifications are concatenated in a tree structure, where each node contains each variable and parameter evaluation. In the end, a combination of different evaluations is performed, allowing it to achieve relevant results for pattern recognition. Considering the sequences of decision related to the Decision Tree method characteristic, its practical implementation and comparison with threshold-based methods becomes easier to be performed, since it can be classified as a threshold method.

For the provision of enough data to learn and train the threshold and machine learning-based algorithms, different approaches are seen in literature. For example, some works employed mannequins wearing the device to perform fall situations. Although this approach allows for the performance of extensive tests (no human risk is involved), the movements are far from real fall movements, since a mannequin will not perform additional movements typically present in a fall (e.g. knees articulation, arms in protective position).

The most common approach for fall detection solutions is the simulation of falls events and ADL performed by volunteers. As this approach offers human risk to the participants involved, they must be done according to approved protocols, where safety measures must be taken to assure as much as possible the integrity of the volunteers. Furthermore, this approach allows for data acquisition of movements that are very similar to falls, increasing the reliability of the algorithms tested on it.

Although the fall and non-fall movements performed in different works mentioned differ between them, avoiding an ideal comparison of results, the most common fall events (e.g. forwards, backwards) are present in most cases. Each researcher is also able to evaluate and identify the weaknesses of a developed algorithm, suggesting fall and ADL simulations that could better train it, in order to achieve a more accurate and reliable solution.

Finally, a cross-validation method is employed in this work to evaluate the best set of parameters for each algorithm (BISHOP, 1995). This evaluation was considered to define the best achieved results for both threshold and machine learning-based methods.

# 3 METHODS

This chapter is divided into five different sections.

The first section presents all the devices and tools related to the data acquisition for algorithms development and evaluation. Also, the approached fall simulation protocols for data acquisition are detailed, presenting their data amount and characteristics.

A second section shows a threshold-based algorithm using two IMU-based sensors. Its approach, development and evaluation process are explored, considering it as an initial evaluation of the fall detection problem.

Then, the third section explains a method for evaluation of the relevance of different variables in fall detection threshold-based algorithms. This evaluation allows a better understanding of how each IMU signal can increase a related fall detector accuracy.

The fourth section explores the Madgwick's algorithm as an improvement factor for fall detection accuracy. In this approach, three IMU-based sensors are used, increasing the information available for the body's spatial orientation. For this reason, it is expected to achieve a better performance in vertical movement definition and, consequently, detection accuracy.

Finally, a last section presents a method for machine learning algorithms evaluation. This analysis is relevant for comparing such a solution with traditional threshold algorithms, allowing a relevant study of fall detection methods for wrist-worn solutions.

## 3.1 DATA ACQUISITION

The development and evaluation of different fall detection algorithms requires a proper amount of IMU-based sensors data. A first possibility to get enough data for proper algorithm development is to search different public data sets, where fall and non-fall signals are available to research. However, depending on how specific the sensors are (including its parameters and configurations), a public data set may be not enough for it, requiring a proper data acquisition. For example, Kwolek e Kepski (2014) recorded a relevant data-set including fall and non-fall

activities, but only image and accelerometer data were acquired. On the other hand, Reiss e Stricker (2012) elaborated a complete dataset with accelerometer, gyroscope and magnetometer data from participants' hand, chest and ankle, but only ADL events were recorded.

In this work, considering the interest for different IMU-based sensors analysis (i.e. accelerometer, gyroscope and magnetometer), allied to a non-usual environment configuration (i.e. a wrist-worn device), a specific protocol for an individual data set was proposed and performed, as follows.

### 3.1.1 ACQUISITION DEVICES AND TOOLS

For the movement signals acquisition, an IMU device (available for sale on internet as GY-80 model) was employed, comprised of a triaxial accelerometer, a triaxial gyroscope, a triaxial magnetometer and a barometer. The barometer was not used, so it will not be detailed in this work. The other three sensors have shown the characteristics below.

The ADXL345 digital accelerometer developed by Analog Devices® (USA) allows a triaxial acceleration measurement in four different ranges (from $\pm 2G$ to $\pm 16G$) with a sample rate up to 3.2kHz. Further, its low power consumption ($23\mu A$ and $0.1\mu A$ in measurement and standby mode, respectively) is a relevant characteristic for embedded systems application (Analog Devices Inc, 2009).

The L3G4200D digital gyroscope developed by ST Microelectronics® (Switzerland) offers a triaxial angular velocity measurement in three different scales: 250, 500 and 2000 degrees per second. Its 16-bit resolution allows a high-quality measurement, with different available sampling rate (from 100Hz to 800Hz), allowing a proper configuration for each application (ST Microelectronics, 2010).

The HMC5883L digital compass developed by Honeywell® (USA) is a triaxial magnetometer able to achieve sampling rates up to 160Hz, with a 12-bit resolution and sensor field range of $\pm 8 Gauss$. Its patented Anisotropic Magnetoresistive (AMR) technology is responsible for increasing the measurement accuracy, making this magnetometer one of the most reliable low-magnetic-field sensors in the industry (HONEYWELL, 2010).

A general property for the three IMU-based sensors described above is the compatible I2C communication protocol feature, allowing a device to configure parameters and read data from them by using only two common wires (beyond power and ground): serial data and serial clock connections. In order to develop this sensor integration and communication quickly, an Arduino UNO development board (Arduino, Italy) was employed. A firmware was developed

to configure all three sensors, reading their data continuously and bypassing this information through a serial port. The acquisition sampling rate employed is 100Hz, since it is the highest sampling rate achieved where no accumulated time delay was empirically observed.

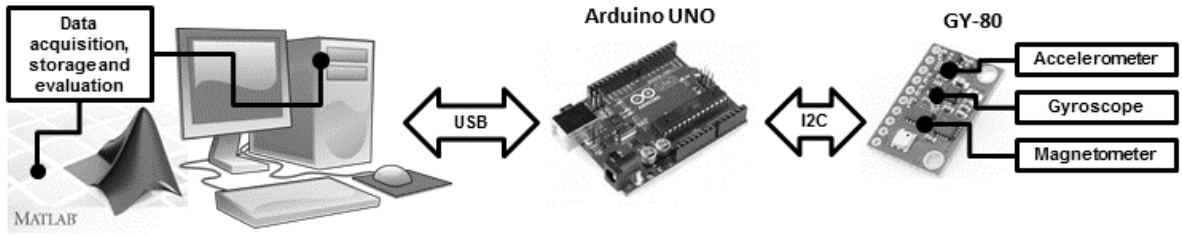


**Figure 6: A diagram related to the employed data acquisition configuration. The data from accelerometer, gyroscope and magnetometer (sensors present on the GY-80 device) are read by an Arduino UNO board and sent to a computer for storage and future evaluation.**

**Source: Own authorship.**

Finally, by the serial port of a personal computer, the IMU device data can be read and submitted to different algorithms developed with a MatLab (MathWorks, USA) platform. In this case, two approaches are available: acquiring and evaluating algorithms in real time data or, differently, acquiring and saving data for posterior analysis. In this work, the acquisition for posterior analysis was chosen, since different algorithms were evaluated for a same data set.

The diagram presented in Figure 6 shows briefly the described configuration for IMU sensors data acquisition and evaluation.

The IMU device and Arduino UNO were assembled into a neoprene watchband, offering a comfortable option for a wrist-worn configuration. The communication between Arduino UNO and the computer was performed through a 5-meter-long USB cable. A solution based on a wireless communication using a Bluetooth adapter was also evaluated. However, in this case, the sampling rate would be limited by the communication speed of the Bluetooth device. So, the USB cable was selected to maximize the available sampling rate. On the other hand, the USB cable restricts the user mobility. So, during all the signal acquisitions, the computer must be placed near to experimental participant position, in order to increase the available area for movement performance.

All the hardware was covered by a hypoallergenic insulation tape, avoiding the risk for electrical shock and other undesirable discomforts during usage. The data acquisition was executed in two different protocols, which were defined during the evolution of the project. In both cases, the data was acquired with 100Hz sampling rate for all sensors with simultaneous acquisition, in a range of 4G for the accelerometer, 500 degrees/sec for the gyroscope and

0.88$Ga$ for the magnetometer. The assembled device is presented in Figure 7.

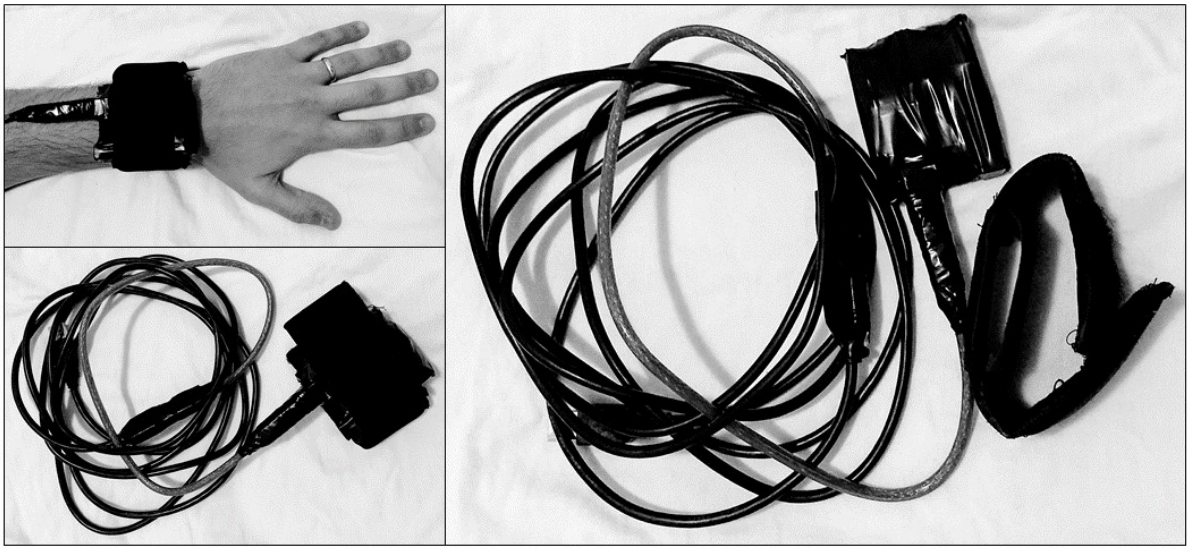

**Figure 7: Employed device for data acquisition. In the photo on the right, the assembled device and the neoprene are presented, disassembled. On the bottom left, the entire system is assembled. On the upper left, a volunteer's wrist using the device is shown.**

**Source: Own authorship.**

### 3.1.2 DATA ACQUISITION PROTOCOLS

In this work, two different protocols were employed. The first protocol considered four fall and four non-fall activities acquired from two experimental participants (researchers involved in the project), and it is referred to in this work as the reduced data acquisition protocol. A second protocol considered six fall and six non-fall activities acquired from twenty-two volunteers, and it is referred to in this work as the complete data acquisition protocol.

The reduced protocol was selected for a general investigation of human movement signals related to fall and non-fall situations. It was also expected to solve the spatial orientation issue requiring the minimum number of sensors. For this reason, only the signals from accelerometer and gyroscope were acquired.

The defined simulation activities for the reduced data acquisition protocol may be found in the Table 2. A single testing cycle consists of a five-time execution for each fall and non-fall activities presented in the table, totaling 40 performed signals. The fall simulation movements were performed on a proper soft mattress, avoiding injuries due to physical impact. The volunteers worn the device at the non-dominant wrist, which reflects a most traditional usage pattern for watches and bands. Also, the non-dominant arm is expected to present lower

physical reflects on fall situations. Table 3 presents the volunteers details.

**Table 2: Reduced data acquisition protocol.**

| Status | Signal |
|---|---|
| Fall | Forward Fall |
| Fall | Backward Fall |
| Fall | Sideways Fall - to the side with the device |
| Fall | Sideways Fall - to the side without the device |
| Non-Fall | Walking |
| Non-Fall | Clapping hands |
| Non-Fall | Closing a door |
| Non-Fall | Sitting on a chair |

**Table 3: Reduced data acquisition volunteers.**

| Index | Gender | Age | Height (m) | Weight (kg) |
|---|---|---|---|---|
| 01 | Male | 27 | 1.71 | 70 |
| 02 | Male | 31 | 1.87 | 75 |

The complete data acquisition protocol was performed under the CAAE identifier code 62000216.0.0000.5547 from the Research Ethics Committee, according to the Resolution 466/2012 from the Brazilian Ministry of Health. As in the reduced protocol, the data was acquired from different volunteers simulating fall and non-fall activities. However, in this case, the magnetometer data was also acquired, leading to a complete information acquisition.

**Table 4: Complete data acquisition protocol.**

| Status | Signal |
|---|---|
| Fall | Forward Fall |
| Fall | Backward Fall |
| Fall | Sideways Fall - to the side with the device |
| Fall | Sideways Fall - to the side without the device |
| Fall | Fall after rotating the waist clockwise |
| Fall | Fall after rotating the waist counterclockwise |
| Non-Fall | Walking |
| Non-Fall | Clapping hands |
| Non-Fall | Opening and closing a door |
| Non-Fall | Moving an object |
| Non-Fall | Tying shoes |
| Non-Fall | Sitting on a chair |

Table 4 presents the testing protocol. The fall movements related to waist rotation intend to simulate falls after the occurrence of mediolateral imbalance (LATASH et al., 2003). In this case, the elderly person may try to see or catch something behind them, but becomes the victim of a fall instead. A single testing cycle consists of a three-times execution for each fall and non-fall activities presented in the table, totaling 36 performed signals.

In the same fashion of the the reduced protocol, all the fall simulation movements were performed on a proper soft mattress to avoid injuries. Also, the volunteers worn the device at the non-dominant wrist. The Figure 8 shows the location where the tests were performed.

For this protocol, twenty-two volunteers were involved, each one performing a single cycle. Each cycle acquisition required about 30 minutes from the volunteers. Thus, a total of 792 signals became available for algorithm development and evaluation; half of those are related to fall simulation, and half to activities of daily life. The Table 5 presents the general characteristics of the volunteers involved.

The 792 acquired signals were then divided into two different data sets: a training set with 600 signals (approximately 75% of all data) and a testing set with the 192 remaining signals. The data used for the training set and for the testing set was randomly chosen, but assuring a same proportion of each movement type from the data acquisition protocol. Thus, the training set and testing set are comprised of 50 and 16 signals, respectively, for each of the twelve different movements defined by the complete data acquisition protocol. These signals were maintained fixed, allowing a proper comparison between the different algorithms.

**Figure 8: Location where the tests were performed. The available mattress is considered ideal for fall experiences.**

**Source: Own authorship.**

The fall and non-fall events simulation does not present exactly the same movement patterns of those performed by elderly people in real life. However, they are the best approximation available for a high number of signal acquisition in a short time, without offering risks

for elderly people. The employed neoprene watchband and the USB cable may also affect the device mechanical characteristics. So, the data acquisition protocol was carefully supervised, in order to reduce the undesirable effects of such a configuration.

**Table 5: Complete data acquisition volunteers.**

| Index | Gender | Age | Height (m) | Weight (kg) |
|---|---|---|---|---|
| 01 | Male | 37 | 1.70 | 70 |
| 02 | Male | 27 | 1.83 | 75 |
| 03 | Male | 28 | 1.58 | 66 |
| 04 | Female | 20 | 1.75 | 78 |
| 05 | Male | 37 | 1.70 | 74 |
| 06 | Female | 20 | 1.57 | 66 |
| 07 | Male | 21 | 1.71 | 76 |
| 08 | Male | 26 | 1.69 | 75 |
| 09 | Male | 23 | 1.80 | 70 |
| 10 | Female | 22 | 1.51 | 45 |
| 11 | Male | 21 | 1.72 | 93 |
| 12 | Male | 23 | 1.78 | 71 |
| 13 | Male | 26 | 1.67 | 67 |
| 14 | Female | 26 | 1.51 | 49 |
| 15 | Male | 24 | 1.69 | 65 |
| 16 | Female | 31 | 1.64 | 56 |
| 17 | Male | 31 | 1.87 | 75 |
| 18 | Male | 26 | 1.89 | 90 |
| 19 | Female | 27 | 1.54 | 53 |
| 20 | Female | 23 | 1.65 | 55 |
| 21 | Female | 28 | 1.53 | 53 |
| 22 | Male | 27 | 1.71 | 70 |

## 3.2 THRESHOLD-BASED METHOD

In the beginning of the project, an initial threshold-based algorithm was developed to investigate how accurate an algorithm could be by acquiring only accelerometer and gyroscope data. Considering an embedded device solution for commercial purposes, the power consumption must be as low as possible. So, the goal was initially to achieve relevant results for a wrist-worn fall detector, using the minimum number of sensors, which would consequently allow a lower power consumption. However, since the literature does not present highly accurate solutions for wrist-worn devices using accelerometer data only (DEGEN et al., 2003; KANG et al., 2006), the gyroscope was employed to offer more spatial orientation data.

The method starts with the accelerometer and gyroscope data acquisition, followed by a simple low-pass filter on acceleration values, which is based on a moving average filter of size

$w_f$ (in this case, $w_f = 40$ and sampling rate is equal to 100Hz). The filter size was selected empirically, in order to present as output a signal very close to the gravity acceleration. This estimated gravity acceleration is relevant for two purposes.

The first purpose is to detect the relative acceleration data. It can be calculated by subtracting the gravity value from the original measured acceleration. This subtraction allows to estimate how much acceleration is present in each accelerometer axis, discarding information related to gravity effect. This is important, because in acceleration threshold analysis, gravity acceleration can be present in any accelerometer axis (due to wrist rotation), becoming an undesirable effect.

The second purpose is to estimate a value which represents the instantaneous movement amount of the device. This value was calculated by subtracting $1G$ ($9.8m/s^2$) from the norm of the three axis components of the low-pass filtered acceleration data. Since $1G$ is the fixed expected value for norm of the gravity acceleration vector, the difference between it and the low-pass filtered acceleration data will be related to the movement intensity of the IMU device. For example, while the device is moving in any direction, even after the low-pass filter, some acceleration additional to gravity is measured. So, the low-pass filtered signal magnitude value will not be exactly $1G$, but a bit higher or lower (depending on the movement's direction), which can be used to calculate a movement intensity.

With this information, the algorithm is able to detect which source is more relevant for the spatial orientation estimation. If the movement intensity is low, the accelerometer information becomes valuable for this calculation. On the other hand, if the movement intensity is high, the use of gyroscope information becomes a more accurate approach. However, two problems are still present when only accelerometer and gyroscope are employed for such purpose, which were also observed in a similar threshold-based algorithm presented by Pierleoni et al. (2016).

The first problem is related to the equations for the spatial orientation. Using the data from accelerometer and gyroscope alone, there is more than one possible solution for the angular equation, related to the gimbal lock effect. In this work, since the spatial orientation relevance for the algorithm is related to the vertical component of the movement, the angular analysis can be limited to a shorter range: $0^\circ$ to $90^\circ$. This approach simplifies the angular equation, allowing the estimation of the IMU device spatial orientation.

The second problem occurs when the measured acceleration is close to zero in one or more axis. In this case, the angular estimation by the accelerometer presents too much noise, avoiding a proper calculation. To solve this problem, the developed algorithm does not consider accelerometer data for the estimation of spatial orientation when values close to zero

are measured, employing gyroscope data instead.

Since the spatial orientation of the IMU device is known, the vertical components of the movement may be calculated. In this work, the vertical component is defined as the direction perpendicular to the floor. For example, while a person is clapping hands, the device would move almost only in the horizontal direction, but while a person hit a table with her hand, the device would move virtually only in the vertical direction. So, the vertical analysis of the movement relies in the vertical displacement expected during a fall.

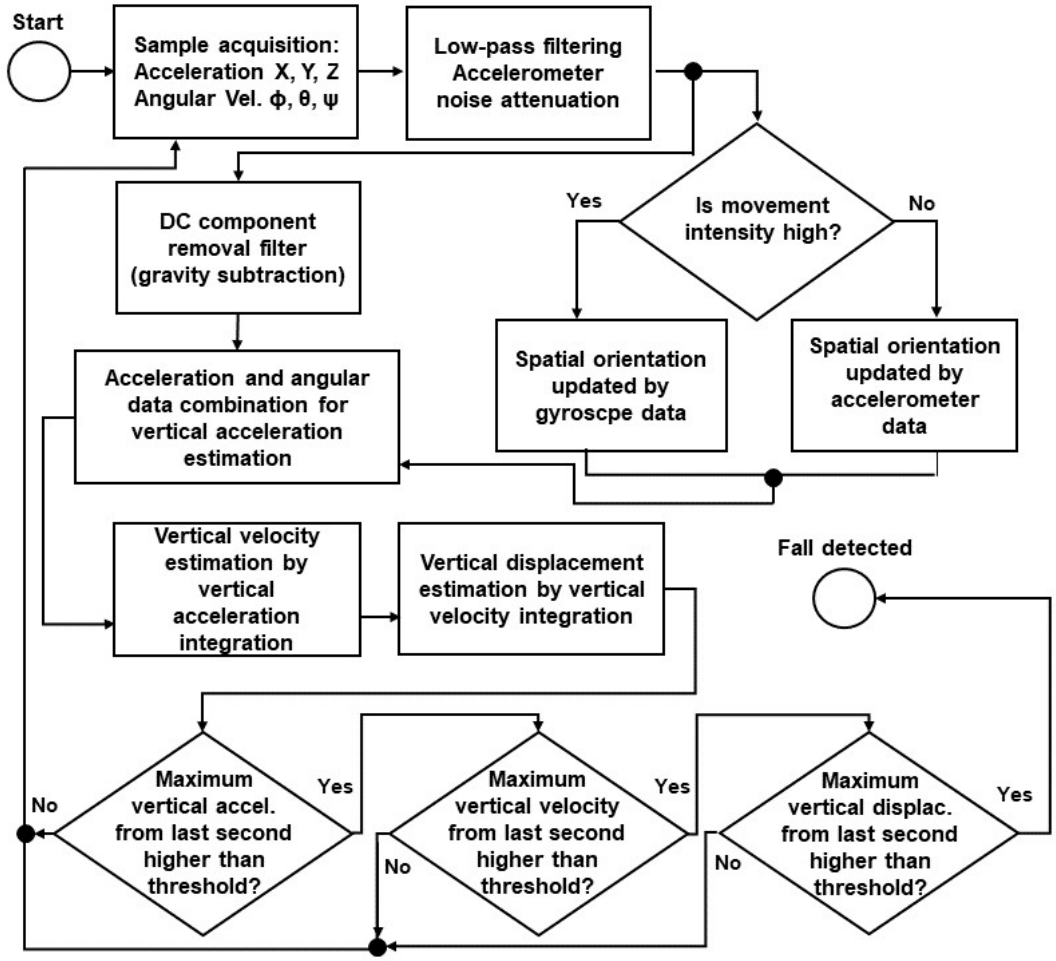


**Figure 9: Proposed threshold-based algorithm flowchart. The method starts with the accelerometer and gyroscope data acquisition, followed by a simple low-pass filter on acceleration values for gravity acceleration estimation. Then, the movement intensity is calculated, in order to identify the best IMU sensor for the estimation of the spatial orientation. So, the vertical acceleration is calculated, which after a single and double integration allows the calculation of the vertical velocity and displacement. Finally, three different threshold analysis are sequentially performed, allowing the detection of a fall event.**

**Source: Own authorship.**

Then, the vertical component of the acceleration data (after the gravity removal, as

explained before) is integrated twice: the first time for the vertical velocity calculation and the second time for the vertical displacement calculation. So, the algorithm receives two additional pieces of information, instead of evaluating only the acceleration data.

An important aspect of the acceleration and velocity integration is the time window integration method. Although a physical definition of velocity and displacement is related to the time integration of acceleration and velocity, respectively, when such calculation is applied in this system, an increasing noise can be seen over time, making the data useless. So, a time window integration of size $w_i$ is applied, where only the last $w_i$ samples are considered into calculation (in this case, $w_i = 100$ and sampling rate is equal to 100Hz).

Finally, a fall event is considered when a vertical displacement is identified, because of a high vertical velocity, and followed by a physical impact. So, three threshold analyses are performed, and the combination of three positive detections within one second is finally considered as a fall event.

Figure 9 presents a flowchart where the method for fall detection is briefly explained. The threshold analyses are performed sequentially, considering one second as the time limit for the complete fall event.

For the training set, the data from two volunteers performing a single cycle of the reduced testing protocol (each one) was evaluated. So, a total of 40 fall and 40 non-fall signals were available for algorithm training. This process is also described in the work presented by Quadros et al. (2016).

Later, after the complete data acquisition protocol became available, a new training process was performed. Then, considering the threshold parameters which achieved the highest accuracy possible, the algorithm was evaluated by the testing set, presenting a final accuracy for the method based on accelerometer and gyroscope configuration.

## 3.3 SIGNALS, PARAMETERS AND THRESHOLDS DEFINITION

After the development of the threshold-based algorithm, an investigation about the relevance of acceleration, velocity and displacement for fall detection algorithms became necessary to understand which configuration for a threshold-based algorithm can present a higher accuracy. Some different possibilities were already shown in Figure 5, in Section 2.5.

For this investigation, an algorithm based on the threshold method previously explained was proposed to evaluate six different signals, as follows:

- Total acceleration (TA): the total acceleration after the removal of gravity;
- Vertical acceleration (VA): similar to TA, but only considering the vertical components of the acceleration;
- Total velocity (TV): the resulting value of the time-window integration of TA;
- Vertical velocity (VV): the resulting value of the time-window integration of VA;
- Total displacement (TD): the resulting value of the time-window integration of TV;
- Vertical displacement (VD): the resulting value of the time window integration of VV;

Furthermore, some parameters may drastically affect the signal values. In order to achieve a complete evaluation of these signals, their configuration parameters must also be investigated. These parameters are:

- Time window for acceleration magnitude (TWAM): the time-window size applied on the first time integration of the acceleration, allowing the selection of the spatial orientation data source (accelerometer or gyroscope);
- Limit for spatial orientation by acceleration (LSOA): the limit value for the acceleration value to consider the accelerometer the best data source for spatial orientation. When this limit is exceeded, the gyroscope is used instead;
- Acceleration time window integration (ATWI): the time-window size applied to the time integration of the acceleration (both TA and VA) to calculate velocity;
- Velocity time window integration (VTWI): the time-window size applied to the time integration of the velocity (both TV and VV) to calculate displacement.

For the parameters' investigation, an evaluation was performed for four different values for TWAM, five for LSOA, five for ATWI and five for VTWI. So, combining all these parameter options, a total of 500 different parameters sets were achieved.

Still, for the threshold evaluation analysis, 500 different thresholds for every one of the six signals was evaluated, starting from a threshold where 100% of sensitivity was achieved and finishing on a threshold where 100% of specificity was achieved. The goal was to identify the best combination of the six signals with different configuration parameters and different thresholds for fall detection.

As six signals were available, there are different combinations of them as well, and each one was evaluated. Firstly, there were six possible combinations for an algorithm analyzing only one signal. They were all evaluated, and the best configuration for both accuracy and sensitivity was registered. Then, using these best configurations, the other combinations were also evaluated: 15 signal combinations for a 2-by-2 set, 20 combinations for a 3-by-3 set, 15 for a 4-by-4 set, 6 for a 5-by-5 and, finally, one single set possible combining all the six signals.

About the data sets, the reduced data acquisition protocol was employed in this evaluation. Firstly, the data from two volunteers (researchers involved in the project) performing a single cycle of the reduced testing protocol was evaluated as a training set. This data is the same one used to train the threshold-based algorithm method, so a total of 40 fall and 40 non-fall signals were available for algorithm training. After that, the best configuration was defined for each signal combination (considering configuration variables, thresholds and time window size), and a final test was performed with a test set, comprised of data from the same two volunteers performing two new cycles of the reduced testing protocol, totaling 80 fall and 80 non-fall signals.

## 3.4 THRESHOLD-BASED METHOD WITH MADGWICK'S ALGORITHM

To evaluate the real contribution of a movement's vertical component in fall detection accuracy, a second method for such a movement's decomposition was evaluated: the algorithm developed by Madgwick et al. (2011). This algorithm uses accelerometer, gyroscope and magnetometer data to calculate the unit quaternion related to the spatial orientation of a body. From this information, the three angles related to the body's spatial orientation ($\phi$, $\theta$, $\psi$) are acquired. Then, this information performs a more robust movement decomposition, employing the accelerometer, gyroscope and magnetometer data fusion.

Through time window integration processes, the vertical velocity and displacement are also estimated. The Figure 10 presents a flowchart related to the employment of Madgwick into previous threshold algorithms, allowing the acquisition of three additional pieces of information. The previous algorithm was adapted to become compatible with Madgwick's algorithm resulting information.

Replacing the movement's vertical components calculated in Section 3.2 by the three values calculated through Madgwick's method, the previous threshold-based algorithms are evaluated again, comparing their performances. However, since magnetometer data was not acquired for the reduced data acquisition protocol, this new method can only be trained and

tested with the complete protocol.

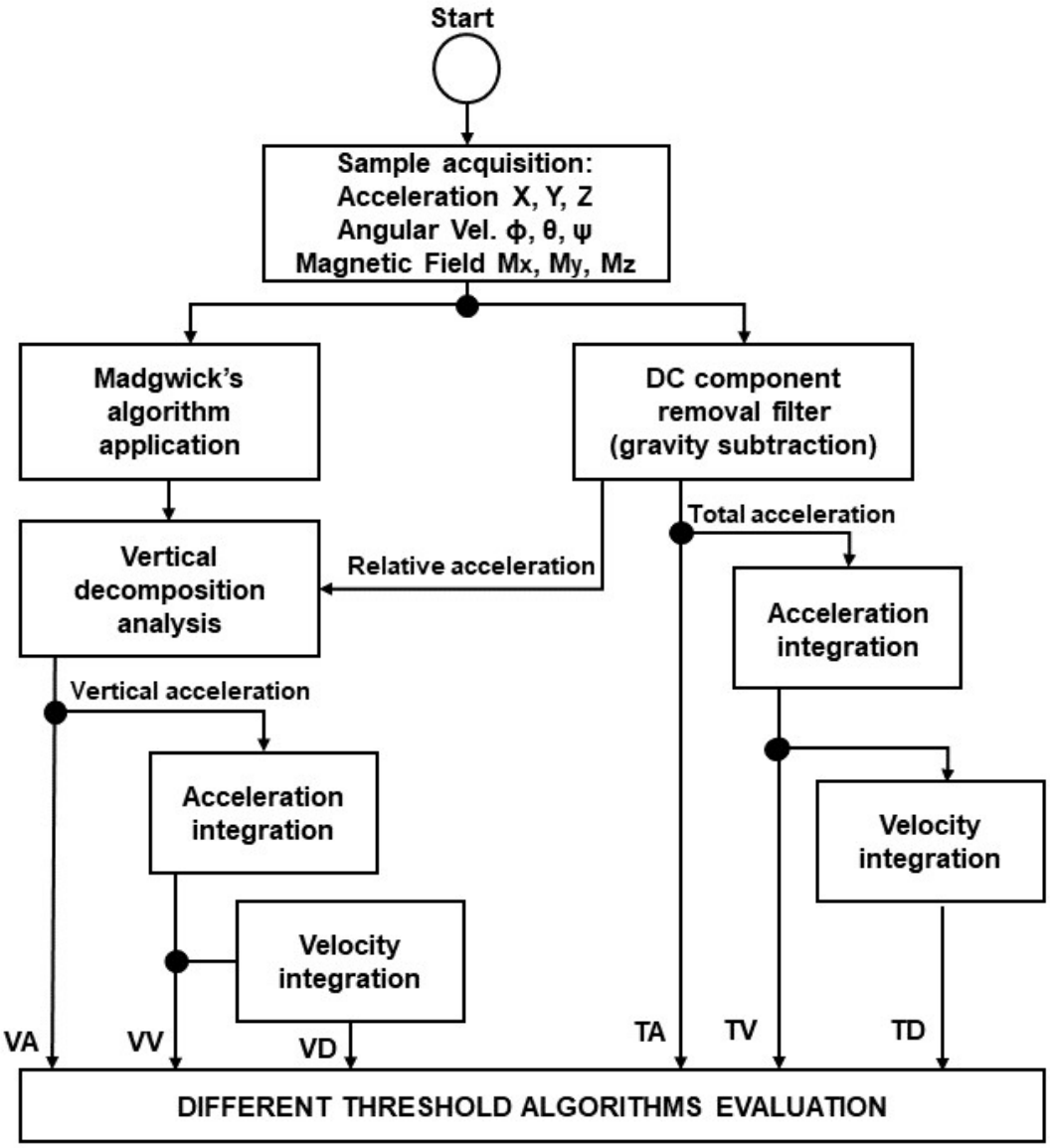


**Figure 10: Flowchart about the threshold algorithm using Madgwick's algorithm. The method starts with the accelerometer, gyroscope and magnetometer data acquisition, which are applied to Madgwick's algorithm for the spatial orientation estimation. A gravity removal filter applied to the original data allows the calculation of the relative acceleration. Combining both information, the vertical acceleration is calculated, which after a single and double integration allows the calculation of the vertical velocity and displacement. So, six different variables become available for threshold evaluation: total and vertical acceleration, velocity and displacement.**

**Source: Own authorship.**

In order to focus on the parameters' configuration which presented the higher accuracy rates for the previous threshold-based methods, the employment of Madgwick's algorithm was evaluated with the same configuration from the initial threshold-based algorithm (VA, VV, VD)

and the algorithms which presented the best results in the evaluation described in Section 3.3. Each configuration was trained and tested again, with the same data sets from the complete data acquisition protocol, allowing a significant comparison between the two methods: with and without magnetometer data.

## 3.5 MACHINE LEARNING

The efficiency of different machine learning methods for fall events detection was also evaluated in this work. The objective of this method was to estimate how accurate a known machine learning algorithm can be for a fall detection solution located at the wrist, beside the comparison with threshold-based methods.

For the machine learning algorithms training and testing, some Matlab ready-for-use libraries developed in the thesis of Lazzaretti (2015) were adapted and applied on the evaluation scenario of this work. Thus, five different machine learning algorithms were approached: K-Nearest Neighbors, Linear Discriminant Analysis, Logistic Regression, Decision Tree and Support Vector Machine.

In order to evaluate the machine learning algorithms according to the available data, the tests were divided into different steps. Firstly, available data from accelerometer was evaluated. Then, data from accelerometer and gyroscope were combined to offer different features (input characteristics) to the system. Finally, the magnetometer data was added to the system, ending the evaluation.

Another relevant aspect about the tests is the data selected for feature extraction: only the vector norm was selected for the machine learning, and not the vectors separately. For example, consider the acceleration *acc* which presents three axes of acceleration ($acc_x$, $acc_y$ and $acc_z$) combined. The machine learning algorithms were not evaluated considering the values of the axes separately, but the vector norm instead. This option was selected for two reasons.

The first reason is to avoid an accurate classification based on specific static positions of the device. Since the movements presented by the test protocol did not consider the use of the device in different initial positions (upside down, for example), an evaluation of the axes separately could offer undesired information for machine learning algorithms. So, working with vector norm, this effect is discarded.

The second reason is related to the comparison of the machine learning algorithms with the threshold-based algorithms, which were developed evaluating a vector norm information. So, considering the vector norm for the machine learning algorithms as well, a comparison

between these methods become more reasonable.

The training and testing sets were taken from the complete data acquisition protocol, totaling 600 signals for training and 192 signals for testing (half to half for fall and non-fall events). These sets were the same applied to the previous threshold-based algorithms.

Initially, considering the accelerometer data only, the selected features were the mean and maximum values of different signals: TA, TV and TD. Also, their combinations were also evaluated: (TA, TV), (TA, TD), (TV, TD) and, finally, (TA, TV, TD). These tests allowed an evaluation of machine learning algorithms when no movement decomposition was applied to the signals.

Then, the tests were performed considering the gyroscope data. The decomposition applied to the threshold-based algorithm was applied to the algorithm, offering new variables for features extraction. So, as in the tests for accelerometer data only, the selected features were the mean and maximum values of the vertical signals: VA, VV and VD. Their combinations were also evaluated: (VA, VV), (VA, VD), (VV, VD) and, finally, (VA, VV, VD).

Finally, the magnetometer information was included in the analysis. Madgwick's algorithm was also employed, offering a more reliable movement decomposition. Thus, the selected features for the machine learning algorithms were the same (mean and maximum values) as for the accelerometer and gyroscope data (VA, VV and VD), but considering the spatial orientation of Madgwick's algorithm. The combination of these signals was also evaluated, as in the previous evaluation.

**Table 6: List of features selected for the machine learning methods.**

| Signals | Features |
|---|---|
| TA | Mean and maximum |
| TV | Mean and maximum |
| TD | Mean and maximum |
| VA | Mean and maximum |
| VV | Mean and maximum |
| VD | Mean and maximum |
| $\phi$ | Mean of sine and cosine |
| $\theta$ | Mean of sine and cosine |
| $\psi$ | Mean of sine and cosine |

Some additional tests were also performed considering the best configurations from threshold-based algorithms analysis. Also, the mean of sine and cosine of the three angles related to the device spatial orientation ($\phi$, $\theta$, $\psi$) were evaluated as features, along with the mean and maximum of the VA, VV and VD values. In this case, a total of twelve features were

evaluated by the algorithms.

Table 6 briefly presents the selected features for the machine learning methods' evaluation. The employed signals were the same used with the threshold-based algorithm.

The results from these tests were compared to the values presented by the threshold-based algorithms, offering the possibility to identify the best approach for fall detection solutions between these two methods.

# 4 RESULTS AND DISCUSSION

In this chapter, the results for each previously described algorithm are presented.

Firstly, the results for the threshold-based algorithm considering the reduced and complete data acquisition protocol are reported, followed by the variable relevance analysis. Then, the relevance of Madgwick's algorithm for threshold-based methods is evaluated. Finally, the results for the different machine learning algorithms are also reported, followed by a final comparison of all the results achieved in this work with those present in the literature.

## 4.1 THRESHOLD-BASED METHOD EVALUATION

The movement decomposition allowed to reduce the influence of non-vertical movements, focusing the threshold analysis only on movements related to height changes. However, even when a movement is totally performed in a non-vertical direction, acceleration is measured in vertical components as noise. This is actually expected, since real movements are not perfectly smooth and show physical vibration, which must be detected as acceleration in all accelerometer axes.

The Figure 11 presents the vertical velocity acquired for two different movements. In the first curve, a volunteer was clapping hands horizontally, the traditional way to clap hands. On the other hand, in the second curve the volunteer was clapping hands vertically, so both hands were moving far and towards the ground, repetitively. The algorithm ability to attenuate non-vertical movements is perceived. Although not all horizontal movement is removed, it is attenuated by at least in 50%.

Further, the vertical velocity and displacement information offers a possibility for increasing system specificity. Since threshold based algorithms related to acceleration-only data are commonly associated to physical impacts, the specificity is decreased when ADL signals with physical impact are evaluated. Thus, the analysis of velocity and displacement seems to contribute, even in a low level, to reduce false positives due to non-vertical movements.

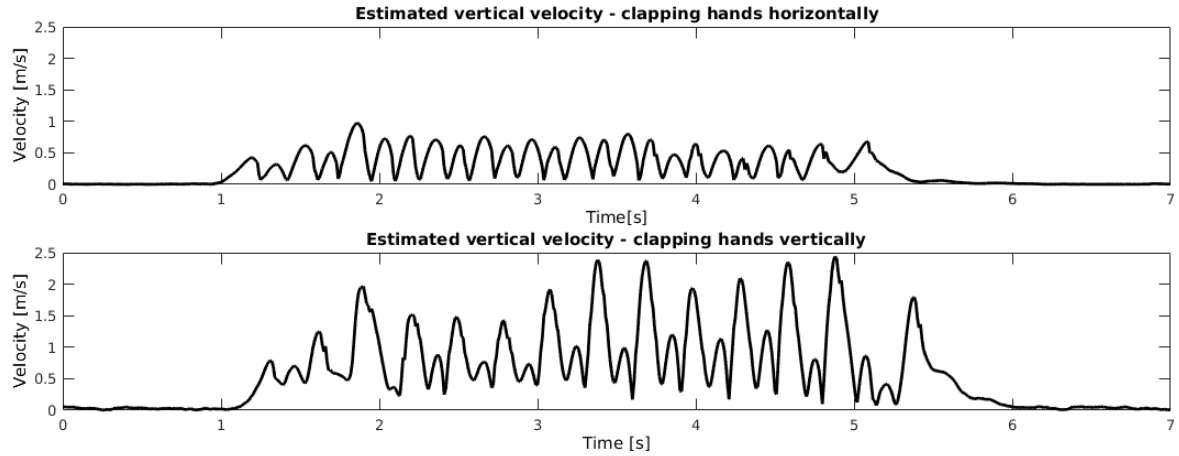


**Figure 11: Vertical velocity acquired for two different movements. In the first case, a volunteer is clapping hands horizontally. In the second, a volunteer is clapping hands vertically.**

**Source: Own authorship.**

The Figure 12 presents calculated velocity and displacement for an acquired non-fall signal. The difference between original and vertical signals helps the proper classification as a non-fall event.

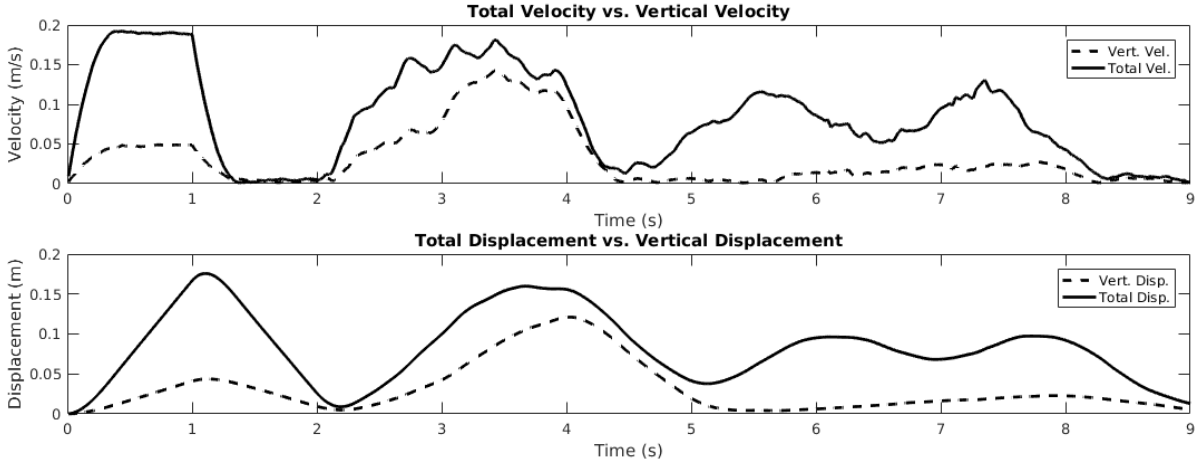


**Figure 12: Velocity and displacement (original and vertical) calculated for a non-fall event. The difference between total and vertical signals is enough to facilitate a threshold algorithm to classify the event properly.**

**Source: Own authorship.**

Evaluating the algorithm with two cycles of the reduced protocol (i.e. 80 different signals), the achieved results are presented in Table 7. Reducing the defined thresholds, the sensibility can be highly increased, but the specificity decreases even more. These results, although far from ideal sensitivity and specificity, are higher than some solutions presented in

literature, justifying the work's significance (DEGEN et al., 2003; KANGAS et al., 2007).

**Table 7: Threshold-based algorithm evaluation for reduced data acquisition protocol.**

| | |
|---|---|
| Total fall signals | 40 |
| Total non-fall signals | 40 |
| True positive | 33 |
| True negative | 29 |
| False positive | 11 |
| False negative | 7 |
| Sensitivity | 82.5% |
| Specificity | 72.5% |
| Accuracy | 77.5% |

These first results for the algorithm were presented in the XXV Brazilian Congress of Biomedical Engineering (CBEB) (QUADROS et al., 2016).

After the complete data acquisition protocol was defined and performed, increasing the available data amount for algorithm development and evaluation, the threshold-based algorithm was trained and tested again. The achieved accuracy value for training set was the highest possible, according to the configuration of different vertical acceleration, velocity and displacement threshold parameters. The results are presented in Table 8. Even training and evaluating the algorithm with a higher amount of data, the accuracy did not change too much, evidencing some consistency for the achieved results.

**Table 8: Threshold-based algorithm evaluation for complete data acquisition protocol.**

| | Training set | Testing set |
|---|---|---|
| Total fall signals | 300 | 96 |
| Total non-fall signals | 300 | 96 |
| True positive | 273 | 83 |
| True negative | 216 | 71 |
| False positive | 84 | 25 |
| False negative | 27 | 13 |
| Sensitivity | 91.0% | 86.5% |
| Specificity | 72.0% | 74.0% |
| Accuracy | 81.5% | 80.2% |

To investigate the relevance of each variable (acceleration, velocity and displacement) and of their vertical component in threshold-based methods, different configurations were evaluated and the results are presented in the next section.

## 4.2 SIGNALS, PARAMETERS AND THRESHOLDS EVALUATION

The exhaustive evaluation of algorithms based on the combination of different signal thresholds and several configuration parameters allowed a robust analysis about the relevance of such signals. The best option for each signal combination was considered the one which presented higher accuracy rate.

Firstly, an evaluation was performed considering a single variable on algorithm analysis. So, six different results were achieved for the learning and training set based on the reduced data acquisition protocol, which are presented in Table 9. The best final result was presented by TV, where a specificity of 77.5% was achieved for a perfect sensitivity.

**Table 9: Comparison of different 1-by-1 algorithms. The evaluation is based on the sensitivity, specificity and accuracy values. The best result is highlighted.**

| | Training Set | | | Testing Set | | |
|---|---|---|---|---|---|---|
| Signal combination | Sens.(%) | Spec.(%) | Acc.(%) | Sens.(%) | Spec.(%) | Acc.(%) |
| TA | 97.5 | 72.5 | 85.0 | 98.8 | 67.5 | 83.1 |
| VA | 92.5 | 72.5 | 82.5 | 93.8 | 70.0 | 81.9 |
| **TV** | **97.5** | **97.5** | **97.5** | **100.0** | **77.5** | **88.8** |
| VV | 100.0 | 92.5 | 96.3 | 92.5 | 53.8 | 73.1 |
| TD | 92.5 | 100.0 | 96.3 | 92.5 | 66.3 | 79.4 |
| VD | 92.5 | 100.0 | 96.3 | 86.3 | 50.0 | 68.1 |

Then, different 2-by-2 signal combination algorithms were evaluated. It is relevant to explain the independence among the different algorithms: the results from the 1-by-1 algorithms could not be considered the ideal for other signal combination algorithms. Although the specificity of the 1-by-1 algorithms may be increased when their configuration and threshold parameters are combined into a 2-by-2 algorithm, for example, the highest sensitivity will always be the lowest of them, or even lower.

So, all the different configuration and threshold parameters need to be evaluated again for each signal combination, in order to identify the best solution for each setup. Table 10 presents the results for the 2-by-2 combination algorithms. The best results were achieved when the VA was combined with TV information: 97.5% of sensitivity and 82.5% of specificity.

Then, the 3-by-3 signal combination was evaluated. Here, the combination (VA, VV, VD) is equivalent to the initial threshold-based algorithm presented in Section 4.1, but since an exhaustive evaluation of different configuration and threshold parameters was performed, a better result was achieved now. However, the best 3-by-3 combination algorithm results were achieved when no vertical analysis was performed: 96.3% of sensitivity and 82.5% of specificity. The results for the 3-by-3 signal combination algorithms are presented in Table 11.

**Table 10: Comparison of different 2-by-2 algorithms. The evaluation is based on the sensitivity, specificity and accuracy values. The best result is highlighted.**

| | Training Set | | | Testing Set | | |
|---|---|---|---|---|---|---|
| Signal combination | Sens.(%) | Spec.(%) | Acc.(%) | Sens.(%) | Spec.(%) | Acc.(%) |
| (TA, VA) | 100.0 | 72.5 | 86.3 | 96.3 | 68.8 | 82.5 |
| **(TA, TV)** | **95.0** | **97.5** | **96.3** | **98.8** | **82.5** | **90.6** |
| (TA, VV) | 100.0 | 92.5 | 96.3 | 92.5 | 75.0 | 83.8 |
| (TA, TD) | 87.5 | 100.0 | 93.8 | 91.3 | 82.5 | 86.9 |
| (TA, VD) | 90.0 | 100.0 | 95.0 | 90.0 | 77.5 | 83.8 |
| (VA, TV) | 97.5 | 97.5 | 97.5 | 97.5 | 82.5 | 90.0 |
| (VA, VV) | 100.0 | 92.5 | 96.3 | 90.0 | 75.0 | 82.5 |
| (VA, TD) | 90.0 | 100.0 | 95.0 | 90.0 | 78.8 | 84.4 |
| (VA, VD) | 92.5 | 100.0 | 96.3 | 87.5 | 76.3 | 81.9 |
| (TV, VV) | 97.5 | 100.0 | 98.8 | 91.3 | 72.5 | 81.9 |
| (TV, TD) | 92.5 | 100.0 | 96.3 | 93.8 | 55.0 | 74.4 |
| (TV, VD) | 95.0 | 97.5 | 96.3 | 97.5 | 67.5 | 82.5 |
| (VV, TD) | 100.0 | 92.5 | 96.3 | 92.5 | 55.0 | 73.8 |
| (VV, VD) | 95.0 | 100.0 | 97.5 | 88.8 | 57.5 | 73.1 |
| (TD, VD) | 90.0 | 100.0 | 95.0 | 90.0 | 70.0 | 80.0 |

**Table 11: Comparison of different 3-by-3 algorithms. The evaluation is based on the sensitivity, specificity and accuracy values. The best result is highlighted.**

| | Training Set | | | Testing Set | | |
|---|---|---|---|---|---|---|
| Signal combination | Sens.(%) | Spec.(%) | Acc.(%) | Sens.(%) | Spec.(%) | Acc.(%) |
| **(TA, VA, TV)** | **95.0** | **97.5** | **96.3** | **96.3** | **82.5** | **89.4** |
| (TA, VA, VV) | 100.0 | 92.5 | 96.3 | 90.0 | 75.0 | 82.5 |
| (TA, VA, TD) | 87.5 | 100.0 | 93.8 | 88.8 | 82.5 | 85.6 |
| (TA, VA, VD) | 90.0 | 100.0 | 95.0 | 86.3 | 77.5 | 81.9 |
| (TA, TV, VV) | 95.0 | 100.0 | 97.5 | 90.0 | 81.3 | 85.6 |
| (TA, TV, TD) | 90.0 | 97.5 | 93.8 | 85.0 | 85.0 | 85.0 |
| (TA, TV, VD) | 87.5 | 100.0 | 93.8 | 90.0 | 82.5 | 86.3 |
| (TA, VV, TD) | 100.0 | 92.5 | 96.3 | 92.5 | 76.3 | 84.4 |
| (TA, VV, VD) | 100.0 | 92.5 | 96.3 | 92.5 | 76.3 | 84.4 |
| (TA, TD, VD) | 85.0 | 100.0 | 92.5 | 88.8 | 82.5 | 85.6 |
| (VA, TV, VV) | 97.5 | 100.0 | 98.8 | 88.8 | 81.3 | 85.0 |
| (VA, TV, TD) | 92.5 | 97.5 | 95.0 | 83.8 | 83.8 | 83.8 |
| (VA, TV, VD) | 90.0 | 100.0 | 95.0 | 87.5 | 82.5 | 85.0 |
| (VA, VV, TD) | 100.0 | 92.5 | 96.3 | 90.0 | 75.0 | 82.5 |
| (VA, VV, VD) | 92.5 | 100.0 | 96.3 | 86.3 | 78.8 | 82.5 |
| (VA, TD, VD) | 92.5 | 95.0 | 93.8 | 96.3 | 76.3 | 86.3 |
| (TV, VV, TD) | 92.5 | 100.0 | 96.3 | 90.0 | 56.3 | 73.1 |
| (TV, VV, VD) | 90.0 | 100.0 | 95.0 | 88.8 | 72.5 | 80.6 |
| (TV, TD, VD) | 90.0 | 100.0 | 95.0 | 91.3 | 56.3 | 73.8 |
| (VV, TD, VD) | 100.0 | 92.5 | 96.3 | 92.5 | 55.0 | 73.8 |

Increasing the number of signals into combination, the 4-by-4 combination algorithms presented similar sensitivity and specificity rates to the 3-by-3 options, as can be observed in Table 12. The best results were achieved by two different signal combinations. Both are comprised of TA, TD and VD signals, but while one of them used vertical acceleration to

increase sensitivity to 96.3%, the other used total velocity to increase specificity to 83.8%. In both cases, the achieved accuracy was 86.9%.

**Table 12: Comparison of different 4-by-4 algorithms. The evaluation is based on the sensitivity, specificity and accuracy values. The best results are highlighted.**

| | Training Set | | | Testing Set | | |
|---|---|---|---|---|---|---|
| Signal combination | Sens.(%) | Spec.(%) | Acc.(%) | Sens.(%) | Spec.(%) | Acc.(%) |
| (TA, VA, TV, VV) | 95.0 | 100.0 | 97.5 | 87.5 | 81.3 | 84.4 |
| (TA, VA, TV, TD) | 90.0 | 97.5 | 93.8 | 81.3 | 85.0 | 83.1 |
| (TA, VA, TV, VD) | 87.5 | 100.0 | 93.8 | 86.3 | 82.5 | 84.4 |
| (TA, VA, VV, TD) | 100.0 | 92.5 | 96.3 | 90.0 | 76.3 | 83.1 |
| (TA, VA, VV, VD) | 100.0 | 92.5 | 96.3 | 90.0 | 76.3 | 83.1 |
| **(TA, VA, TD, VD)** | **92.5** | **95.0** | **93.8** | **96.3** | **77.5** | **86.9** |
| (TA, TV, VV, TD) | 97.5 | 92.5 | 95.0 | 92.5 | 78.8 | 85.6 |
| (TA, TV, VV, VD) | 97.5 | 92.5 | 95.0 | 92.5 | 77.5 | 85.0 |
| **(TA, TV, TD, VD)** | **95.0** | **92.5** | **93.8** | **90.0** | **83.8** | **86.9** |
| (TA, VV, TD, VD) | 100.0 | 92.5 | 96.3 | 92.5 | 76.3 | 84.4 |
| (VA, TV, VV, TD) | 90.0 | 100.0 | 95.0 | 83.8 | 83.8 | 83.8 |
| (VA, TV, VV, VD) | 90.0 | 100.0 | 95.0 | 86.3 | 82.5 | 84.4 |
| (VA, TV, TD, VD) | 95.0 | 92.5 | 93.8 | 87.5 | 82.5 | 85.0 |
| (VA, VV, TD, VD) | 100.0 | 92.5 | 96.3 | 90.0 | 75.0 | 82.5 |
| (TV, VV, TD, VD) | 90.0 | 100.0 | 95.0 | 88.8 | 56.3 | 72.5 |

**Table 13: Comparison of different 5-by-5 and 6-by-6 algorithms. The evaluation is based on the sensitivity, specificity and accuracy values. The best results are highlighted.**

| | Training Set | | | Testing Set | | |
|---|---|---|---|---|---|---|
| Signal combination | Sens.(%) | Spec.(%) | Acc.(%) | Sens.(%) | Spec.(%) | Acc.(%) |
| (TA, VA, TV, VV, TD) | 97.5 | 92.5 | 95.0 | 90.0 | 78.5 | 84.3 |
| (TA, VA, TV, VV, VD) | 97.5 | 92.5 | 95.0 | 90.0 | 77.5 | 83.8 |
| **(TA, VA, TV, TD, VD)** | **95.0** | **92.5** | **93.8** | **87.5** | **83.8** | **85.6** |
| (TA, VA, VV, TD, VD) | 100.0 | 92.5 | 96.3 | 90.0 | 76.3 | 83.1 |
| **(TA, TV, VV, TD, VD)** | **97.5** | **92.5** | **95.0** | **92.5** | **78.8** | **85.6** |
| (VA, TV, VV, TD, VD) | 97.5 | 92.5 | 95.0 | 90.0 | 77.5 | 83.8 |
| (TA, VA, TV, VV, TD, VD) | 97.5 | 92.5 | 95.0 | 90.0 | 78.8 | 84.4 |

Finally, the Table 13 presents the results for the 5-by-5 and 6-by-6 combination. In this case, all the algorithms presented very similar results, and no combination can be highlighted.

From all the results, the four highest achieved accuracy rates are presented in Table 14. The displacement is not present in the list, reducing its relevance on the proposed fall detection algorithm. On the other hand, velocity is present in all of them, reinforcing its relevance for fall detection algorithms, as already presented in the literature (WU, 2000; DEGEN et al., 2003).

These results related to the evaluation of different variables' relevance in a fall detection algorithm were presented in the VII Latin American Congress in Biomedical Engineering (CLAIB) (QUADROS et al., 2017).

**Table 14: The top four configurations for signal combination. The evaluation is based on the sensitivity, specificity and accuracy values. The best result is highlighted.**

| | Training Set | | | Testing Set | | |
|---|---|---|---|---|---|---|
| Signal combination | Sens.(%) | Spec.(%) | Acc.(%) | Sens.(%) | Spec.(%) | Acc.(%) |
| **(TA, TV)** | **95.0** | **97.5** | **96.3** | **98.8** | **82.5** | **90.6** |
| (VA, TV) | 97.5 | 97.5 | 97.5 | 97.5 | 82.5 | 90.0 |
| (TA, VA, TV) | 95.0 | 97.5 | 96.3 | 96.3 | 82.5 | 89.4 |
| (TV) | 97.5 | 97.5 | 97.5 | 100.0 | 77.5 | 88.8 |

After the complete data acquisition protocol was defined and performed, some algorithms from the method were trained (only the threshold values) and tested again, to evaluate the consistency of the first results. For this evaluation, the top four signal combinations presented in Table 14 were evaluated. Additionally, the configuration related to the initial threshold-based algorithm (VA, VV, VD) was also evaluated, as a comparison with the results presented in Section 4.1.

So, the Table 15 presents the results for these signal combination algorithms for the complete data acquisition protocol. The achieved accuracy rates are a bit lower than those presented with the reduced protocol. The combination of total acceleration and total velocity keeps showing the best results: 95.8% of sensitivity and 82.3% of specificity. About the signal combination related to the initial threshold-based algorithm presented in Section 4.1, the achieved results were surprisingly better than before, which can be explained by a better configuration of threshold parameters for every signal.

**Table 15: Evaluation of different signal combination algorithms with the complete data acquisition protocol. The evaluation is based on the sensitivity, specificity and accuracy values. The best result is highlighted.**

| | Training Set | | | Testing Set | | |
|---|---|---|---|---|---|---|
| Signal combination | Sens.(%) | Spec.(%) | Acc.(%) | Sens.(%) | Spec.(%) | Acc.(%) |
| **(TA, TV)** | **97.7** | **81.7** | **89.7** | **95.8** | **82.3** | **89.1** |
| (VA, TV) | 94.3 | 82.0 | 88.2 | 91.7 | 82.3 | 87.0 |
| (TA, VA, TV) | 95.0 | 82.7 | 88.8 | 93.8 | 83.3 | 88.5 |
| (TV) | 92.7 | 79.0 | 85.8 | 86.5 | 80.2 | 83.3 |
| (VA, VV, VD) | 94.0 | 72.0 | 83.0 | 95.8 | 72.9 | 84.4 |

These results help a better understanding of how each variable may contribute in fall detection algorithms accuracy. Also, the fact that vertical components of acceleration and velocity are not present in the best results list suggests such an effort in movement decomposition is non relevant. However, since the movement decomposition proposed is based only on accelerometer and gyroscope data, the results for vertical components of movement may not be the ideal, and a better evaluation can be done through the employment of a magnetometer device and Madgwick's algorithm.

## 4.3 MADGWICK'S ALGORITHM EMPLOYMENT EVALUATION

For the threshold-based method with Madgwick's algorithm employment, magnetometer data is a required information. For this reason, this method could not be trained and evaluated by the reduced data acquisition protocol. However, since the previous algorithms were also trained and tested with the complete data acquisition protocol, a comparison between them is still possible.

Madgwick's algorithm was expected to increase reliability on movement decomposition. Figure 13 shows an example of Madgwick's algorithm relevance. For a non-fall signal, where less vertical movement is involved, the calculated vertical velocity must present lower values than total. Comparing with the method using accelerometer and gyroscope only, it is possible to see this effect. On the other hand, when a fall signal is evaluated, the vertical component of the movement is expected to be highlighted. According to the figure, it also presented a better result than previous accelerometer and gyroscope-only methods.

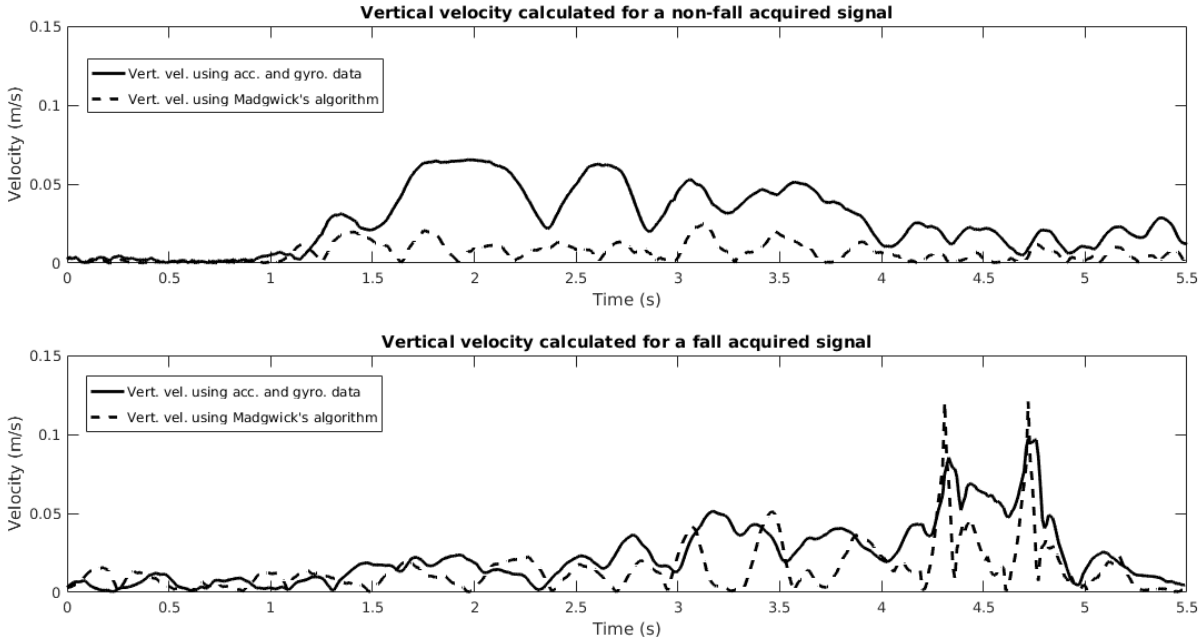


**Figure 13: Comparison between accelerometer and gyroscope movement decomposition with Madgwick's algorithm. Two different signals were evaluated: one related to a fall event, and other related to a non-fall event. Madgwick's algorithm attenuates non-fall events better than the algorithm based on accelerometer and gyroscope data only.**

**Source: Own authorship.**

In order to evaluate the possibility of increasing fall detection accuracy by combining threshold-based algorithms with Madgwick's method for spatial orientation calculation, all the configurations presented in Table 15 (best results of this work for threshold-based algorithms

employing accelerometer and gyroscope data) which are related to vertical analysis were trained and tested.

Initially, the combination VA and TV was evaluated. The results for training set and testing set are presented in Table 16. Comparing it with the best algorithm results previously achieved (TA, TV), it is possible to observe an equal sensitivity, but a higher specificity. When comparing it to the same configuration for the previous algorithm (without Madgwick's method), the accuracy was increased from 87.0% to 91.1%.

**Table 16: Threshold-based method with Madgwick's algorithm evaluation for complete data acquisition protocol with (VA, TV) configuration.**

| | Training set | Testing set |
|---|---|---|
| Total fall signals | 300 | 96 |
| Total non-fall signals | 300 | 96 |
| True positive | 285 | 92 |
| True negative | 256 | 83 |
| False positive | 44 | 13 |
| False negative | 15 | 4 |
| Sensitivity | 95.0% | 95.8% |
| Specificity | 85.3% | 86.5% |
| Accuracy | 90.2% | 91.1% |

Then, the algorithm was trained and tested with the (TA, VA, TV) configuration. The achieved results were exactly the same than those presented in Table 16. That happened because the TA information did not add any relevant information to the algorithm that was not already shown by VA and TV. So, it was not able to increase either sensitivity or specificity.

**Table 17: Threshold-based method with Madgwick's algorithm evaluation for complete data acquisition protocol with (VA, VV, VD) configuration, the same one used in initial threshold-based algorithm.**

| | Training set | Testing set |
|---|---|---|
| Total fall signals | 300 | 96 |
| Total non-fall signals | 300 | 96 |
| True positive | 279 | 92 |
| True negative | 234 | 77 |
| False positive | 66 | 19 |
| False negative | 21 | 4 |
| Sensitivity | 93.0% | 95.8% |
| Specificity | 78.0% | 80.2% |
| Accuracy | 85.5% | 88.0% |

Finally, the same configuration approached in the initial threshold-based algorithm (VA, VV, VD) was trained and tested again, in order to evaluate the evolution of this combination. The results are presented in Table 17. The achieved accuracy rate was 88%, a bit higher

than the 84.4% achieved in the best case for the previous algorithm. Similar to the (VA, TV) combination results, Madgwick's algorithm did not present an increase in sensitivity, but only in specificity rate.

Despite the improvement on the fall detection accuracy, Madgwick's algorithm was not able to allow the proposed threshold method to achieve an ideal sensitivity and specificity. Even employing the magnetometer data, the highest accuracy achieved was 91.1%.

## 4.4 MACHINE LEARNING

The machine learning methods' evaluation was divided into the different steps presented in Section 3.5.

Initially, considering the accelerometer as the only source of information, the five different machine learning methods were trained and tested. The best results are presented in Table 18. For four machine learning methods, the best results occurred when the mean and maximum values of the total acceleration, velocity and displacement were selected as features. A possibility for this is the fact that this configuration is the one which presents more information (6 features) from all the configurations tested in this initial evaluation.

**Table 18: Best machine learning results for accelerometer-only data. The presented values are related to testing set evaluation. The best result is highlighted.**

| | K-Near. Neigh. | LDA | **Log. Reg.** | Dec. Tree | SVM |
|---|---|---|---|---|---|
| Configuration | (TA,TV,TD) | (TA,TV,TD) | **(TA,TV,TD)** | (TA,TV,TD) | (TA,TD) |
| True positive | 91 | 92 | **94** | 90 | 91 |
| True negative | 88 | 91 | **92** | 88 | 94 |
| False positive | 8 | 5 | **4** | 8 | 2 |
| False negative | 5 | 4 | **2** | 6 | 5 |
| Sensitivity | 94.8% | 95.8% | **97.9%** | 93.8% | 94.8% |
| Specificity | 91.7% | 94.8% | **95.8%** | 91.7% | 97.9% |
| Accuracy | 93.2% | 95.3% | **96.9%** | 92.7% | 96.4% |

Another interesting point is the high accuracy of the Logistic Regression method, presenting 97.9% and 95.8% of sensitivity and specificity, respectively. These results are considerably better than those presented by all the threshold-based algorithms, and required data only from the accelerometer.

Then, the vertical decomposition by accelerometer and gyroscope was evaluated. The best results for the five machine learning methods are presented in Table 19. They are worse than those achieved when only the accelerometer data was employed. It happened because the movement decomposition applied to the signals reduced the possibility for a pattern recognition

by removing some relevant feature characteristics for the machine learning methods classification (e.g. difference among mean values of the fall and non-fall signals), leading to a detection accuracy decrease.

The best case was presented by the SVM method: 92.7% of sensitivity and 97.9% of specificity, leading to an accuracy of 95.3%. This result is also higher than those presented by the threshold-based algorithms.

**Table 19: Best machine learning results for accelerometer and gyroscope data. The values presented are related to testing set evaluation. The best result is highlighted.**

| | K-Near. Neigh. | LDA | Log. Reg. | Dec. Tree | **SVM** |
|---|---|---|---|---|---|
| Configuration | (VA,VD) | (VA,VV,VD) | (VA,VV,VD) | (VA,VD) | **(VA,VD)** |
| True positive | 89 | 88 | 88 | 87 | **89** |
| True negative | 87 | 87 | 89 | 88 | **94** |
| False positive | 9 | 9 | 7 | 8 | **2** |
| False negative | 7 | 8 | 8 | 9 | **7** |
| Sensitivity | 92.7% | 91.7% | 91.7% | 90.6% | **92.7%** |
| Specificity | 90.6% | 90.6% | 92.7% | 91.7% | **97.9%** |
| Accuracy | 91.7% | 91.1% | 92.2% | 91.1% | **95.3%** |

Then, the magnetometer influence in machine learning methods' accuracy was evaluated. As in the features evaluated for the accelerometer and gyroscope configuration, new tests were performed using the information acquired from Madgwick's algorithm, allowing us to achieve the results presented in Table 20.

**Table 20: Best machine learning results for accelerometer, gyroscope and magnetometer data. The configuration variables between brackets [] can be removed without affecting the final result. The presented values are related to testing set evaluation. The best result is highlighted.**

| | **K-Near. Neigh.** | LDA | Log. Reg. | Dec. Tree | SVM |
|---|---|---|---|---|---|
| Configuration | **(VA,VV,[VD])** | (VA,VV) | (VA,VV) | (VA,VD) | (VA,VD) |
| True positive | **93** | 92 | 91 | 90 | 91 |
| True negative | **92** | 82 | 86 | 91 | 93 |
| False positive | **4** | 14 | 10 | 5 | 3 |
| False negative | **3** | 4 | 5 | 6 | 5 |
| Sensitivity | **96.9%** | 95.8% | 94.8% | 93.8% | 94.8% |
| Specificity | **95.8%** | 85.4% | 89.6% | 94.8% | 96.9% |
| Accuracy | **96.4%** | 90.6% | 92.2% | 94.3% | 95.8% |

In this evaluation, K-Nearest Neighbors and Decision Tree methods achieved better results than those achieved when sensors' data was employed. The other methods did not present relevant changes in accuracy when compared with the results presented in Table 19. The best case was presented by the K-Nearest Neighbors method when the mean and maximum of vertical acceleration and velocity were selected as features, where sensitivity and specificity rates higher than 95% was achieved.

Finally, additional tests were performed for three more configurations. The first one was the evaluation of the sine and cosine means from the three angles related to the device's spatial orientation ($\phi$, $\theta$, $\psi$). These values were added as features to the already evaluated combination (VA, VV, VD). In this, twelve features became evaluated by the machine learning methods. The other two configurations are related to the best cases presented by the threshold-based algorithms which were not previously tested by the machine learning methods. So, the mean and maximum values from (VA, TV) and (TA, VA, TV) were selected as features.

The best results from these three configurations for each machine learning method are presented in Table 21. These are also the best results for each method among all the results presented for the machine learning evaluation.

**Table 21: An additional analysis for best machine learning results for accelerometer, gyroscope and magnetometer data. The presented values are related to testing set evaluation. The best result is highlighted.**

| | **K-Near. Neigh.** | LDA | Log. Reg. | Dec. Tree | SVM |
|---|---|---|---|---|---|
| Configuration | **+Angles** | (TA,VA,TV) | (VA,TV) | (VA,TV) | (VA,TV) |
| True positive | **96** | 95 | 94 | 94 | 94 |
| True negative | **94** | 90 | 93 | 90 | 93 |
| False positive | **2** | 6 | 3 | 6 | 3 |
| False negative | **0** | 1 | 2 | 2 | 2 |
| Sensitivity | **100.0%** | 99.0% | 97.9% | 97.9% | 97.9% |
| Specificity | **97.9%** | 93.8% | 96.9% | 93.8% | 96.9% |
| Accuracy | **99.0%** | 96.4% | 97.4% | 95.8% | 97.4% |

The angular information appeared to be more relevant for K-Nearest Neighbors method, allowing it to achieve 100% and 97.9% of sensitivity and specificity, respectively. Logistic Regression and SVM methods also presented relevant results: both achieved 97.4% of accuracy. LDA and Decision Tree methods presented considerably better than those achieved by the threshold-based algorithms evaluated in this work as well.

Many other signal combinations are possible to be investigated. However, such an evaluation is not part of the scope of this work. Furthermore, the goal of 100% of sensitivity and specificity of 95% or higher was already achieved by the K-Nearest Neighbors method, and many other results for the machine learning methods also presented sensitivity and specificity rates much higher than those achieved by the threshold-based algorithms, becoming the main method used in this work for fall events classification.

## 4.5 COMPARISON AND DISCUSSION

Since all the algorithms presented in this work were trained and tested by the same training and testing set from the complete data acquisition protocol, it is possible to perform a comparison of all the employed algorithms. Also, the results achieved by solutions from the literature, which were presented in Section 2.3, allow an evaluation of the contribution of this work.

For the threshold-based algorithms, different configurations were measured, considering data from different sensors. It allowed an evolution of this method, which can be evidenced by an increase in the achieved accuracy between the first threshold-based algorithm (considering accelerometer and gyroscope data) and the last one (considering the magnetometer information, as well). These results are presented in Table 22, where the improvement is perceived in both sensitivity and specificity rates.

**Table 22: Evolution of the threshold-based (TH) algorithms developed in this work. The final threshold-based algorithm additionally employs the magnetometer data, instead of accelerometer and gyroscope data only.**

| | Initial TH algorithm | Final TH algorithm |
|---|---|---|
| Sensors | Acc. and gyro. | Acc., gyro. and magnet. |
| Configuration | (VA, VV, VD) | (VA, TV) |
| Sensitivity | 86.5% | 95.8% |
| Specificity | 74.0% | 86.5% |
| Accuracy | 80.2% | 91.1% |

However, the machine learning algorithms achieved even better results than those achieved by the threshold-based algorithms. A comparison between the two best cases for threshold-based and machine learning algorithms is presented in Table 23. In both cases, data from accelerometer, gyroscope and magnetometer were employed.

**Table 23: Comparison of the best results achieved for threshold-based (TH) and machine learning (K-Nearest Neighbors) algorithms.**

| | Best TH algorithm | K-Near. Neigh. algorithm |
|---|---|---|
| Sensors | Acc., gyro. and magnet. | Acc., gyro. and magnet. |
| Configuration | (VA, TV) | Features from (VA, VV, VD, $\phi$, $\theta$, $\psi$) |
| Sensitivity | 95.8% | 100.0% |
| Specificity | 86.5% | 97.9% |
| Accuracy | 91.1% | 99.0% |

An interesting approach for comparing these results with those present in the literature is based on the evaluation of the sensors used in such solutions, considering an equal data

availability. Another relevant point concerns the testing protocols approached in the literature. Since they are different for each solution, only an approximate comparison is possible.

Thus, starting a comparison with the solutions based on accelerometer data only, the Table 1 presented in Section 2.3 may be adapted for the solutions with this configuration, as can be seen in Table 24.

Kangas et al. (2007), Bourke et al. (2007) and Tong et al. (2013) already achieved ideal results for a fall detection solution, but considering sensors worn at the head and the trunk. For wrist-worn solutions, Degen et al. (2003) achieved 65% of accuracy using a threshold-based algorithm, while Yuan et al. (2015) achieved an accuracy of 94.3% using machine learning methods.

**Table 24: Comparison of different fall detection solutions presented in literature, considering only accelerometer information. The methods are distinguished between threshold-based (TH) and machine learning (ML).**

| Reference | Method | Configuration | Best results |
|---|---|---|---|
| (DEGEN et al., 2003) | TH | Wrist | AC: 65% |
| (KANG et al., 2006) | TH | Wrist | SE: 91.3% |
| (KANGAS et al., 2007) | TH | Waist, head and wrist | Head – AC: 100% |
| (BOURKE et al., 2007) | TH | Thigh and trunk | Trunk – AC: 100% |
| (BAGNASCO et al., 2011) | TH | Waist, chest, wrist | Chest – SE:88% SP:100% |
| (CHENG; JHAN, 2013) | ML | Ankle, chest, waist | Waist – AC: 98.48% |
| (TONG et al., 2013) | ML | Trunk | AC: 100% |
| (KAMBHAMPATI et al., 2015) | ML | Waist | AC: 96.91% |
| (YUAN et al., 2015) | ML | Wrist | AC: 94.3% |
| (CONCEPCION et al., 2016) | TH | Waist | AC: 95% |
| (PANNURAT et al., 2017) | ML | Many | Waist - AC: 91,15% |
| (AZIZ et al., 2017) | TH/ML | Waist | AC: 96% |

Not all papers present in the literature reported the achieved accuracy of their methods. In such cases, a comparison becomes incomplete, complicating a proper evaluation of the performance of these algorithms.

**Table 25: Comparison of the best results achieved for threshold-based (TH) and machine learning (Logistic Regression) algorithms, considering only accelerometer information.**

| | TH algorithm | Log. Regression algorithm |
|---|---|---|
| Configuration | (TA, TV) | Features from (TA, TV, TD) |
| Sensitivity | 95.8% | 97.9% |
| Specificity | 82.3% | 95.8% |
| Accuracy | 89.1% | 96.9% |

The best results for the algorithms developed in this work employing accelerometer data are presented in Table 25. The threshold-based algorithm achieved considerably better

results than those presented by Degen et al. (2003). On the other hand, the developed Logistic Regression algorithm achieved a very similar accuracy to the solution presented by Yuan et al. (2015), which was also based on a wrist-worn device.

Similarly, considering the methods available in the literature based on accelerometer and gyroscope data, some interesting results are presented in Table 26.

For this configuration, no solution based on a wrist-worn device was observed in the literature. Liu e Lockhart (2014) achieved great results considering the device worn at the trunk. Similarly, Lee et al. (2015) achieved a high accuracy for a device located at the waist. In both cases, a threshold-based method was approached.

**Table 26: Comparison of different fall detection solutions presented in literature, considering accelerometer and gyroscope information. The methods are distinguished between threshold-based (TH) and machine learning (ML).**

| Reference | Method | Configuration | Best results |
|---|---|---|---|
| (LIU; LOCKHART, 2014) | TH | Trunk | SE: 100% SP: 95.65% |
| (LEE et al., 2015) | TH | Waist | AC: 95% |
| (VALCOURT et al., 2016) | TH | Undefined | AC: 81.3% |
| (ANDO et al., 2016) | ML | Waist | SE: 81% SP: 98% |

The only solution from this group based on a machine learning method was presented by Ando et al. (2016). However, in their work, different movement patterns were considered for machine learning classification, and not fall and non-fall events only. So, although their achieved results are not as good as those presented by Liu e Lockhart (2014), they concern a more complex pattern recognition evaluation.

The best results for the algorithms developed in this work employing accelerometer and gyroscope data are presented in Table 27. The movement decomposition based on accelerometer and gyroscope data was not efficient on increasing the fall detection accuracy. Actually, the achieved results for this configuration were even worse than those achieved employing only accelerometer data.

**Table 27: Comparison of the best results achieved for threshold-based (TH) and machine learning (SVM) algorithms, considering accelerometer and gyroscope information.**

| | TH algorithm | SVM algorithm |
|---|---|---|
| Configuration | (VA, TV) | Features from (VA, VD) |
| Sensitivity | 91.7% | 92.7% |
| Specificity | 82.3% | 97.9% |
| Accuracy | 87.0% | 95.3% |

On the other hand, the results presented in the literature using accelerometer and gyroscope data show an evolution of the IMU-based fall detection methods when compared to those

related to accelerometer data only. These great results may be justified by the lower number of degrees of freedom presented by the waist and trunk positions. In such configurations, the spatial orientation may be calculated through a simpler approach, where the accelerometer and gyroscope can be considered enough source of information.

Finally, considering the employment of the accelerometer, gyroscope and magnetometer sensors, the only solution found in literature was proposed by Pierleoni et al. (2015). In their work, a threshold-based algorithm was developed, and an accuracy of 90.37% was achieved. This result was not so relevant when compared to those presented in Table 26. An evolution of their work employed a barometer as an additional information source, allowing the achievement of 99.8% of accuracy (PIERLEONI et al., 2016). In both cases, the method considered an IMU device worn at the waist.

The best results for the algorithms developed in this work employing accelerometer, gyroscope and magnetometer data are presented in Table 28.

**Table 28: Comparison of the best results achieved for threshold-based (TH) and machine learning (K-Nearest Neighbors) algorithms, considering accelerometer, gyroscope and magnetometer information.**

| | TH algorithm | K-Near. Neigh. algorithm |
|---|---|---|
| Configuration | (VA, TV) | Features from (VA, VV, VD + Angles) |
| Sensitivity | 95.8% | 100.0% |
| Specificity | 86.5% | 97.9% |
| Accuracy | 91.1% | 99.0% |

Comparing the threshold-based method results with those presented by Pierleoni et al. (2015), a similar accuracy was achieved, but for a system worn in different places of the body. On the other hand, the results achieved by the machine learning methods were considerably better than many other results present in the literature. This may be justified by the employment of three sensors (accelerometer, gyroscope and magnetometer) in a machine learning approach, allowing a higher amount of gathered information than the methods approached in Table 26, even for a wrist-worn configuration.

After all the performed tests, threshold-based algorithms did not present enough accuracy to solve the proposed fall detection accuracy problem, but the machine learning methods did. For this reason, future works related to wrist-worn fall detectors should be focused in machine learning approaches to achieve better results.

# 5 CONCLUSION

This work presented the elderly falls as a serious problem, which reduces the life quality of many elderly people and their families around the world. In this scenario, a fall detection system becomes relevant, offering an improvement of life's quality for elderly people.

So, considering the results obtained during this work development, the complexity of a fall detector based on a wrist located device was evidenced. Since a human wrist is able to perform too many different movements, its spatial orientation calculation becomes much more complicated than other human body positions, as the chest, neck or waist. For this reason, threshold based algorithms, which could offer great accuracy for chest or waist worn fall detectors, presents unsatisfactory results for a wrist worn configuration.

The results allowed to conclude that a higher amount of information may considerably increase the fall detection accuracy. In other words, a fall detection algorithm based on information from three sensors (accelerometer, gyroscope and magnetometer) presented more relevant results than those based on only one sensor. This conclusion was already perceived by some works in the literature, and its relevance for the proposed wrist worn fall detector was reliably showed. For example, considering all the evaluated algorithms, the best accuracy for a solution based on accelerometer data only was 96.9%, while for a three sensors system, the achieved accuracy was 99%.

Different threshold based algorithms were evaluated as an option to solve the fall detection problem using a wearable device located at wrist. Also, different machine learning methods were also evaluated, allowing a comparison between these two approaches for a same data set. Further, the achieved results for both methods were also compared to those present in the literature. This comparison may not be considered ideal, since each work employed a different protocol for algorithms training and testing. However, such a comparison is still relevant, allowing the identification of advantages and disadvantages of different fall detection approaches.

This work did not evaluate options for friends and family notification. There are several

low-consumption options to perform this notification, as the use of Bluetooth communication between the device and a central gateway, which could notify family members by phone or internet. However, this work remained focused on developing and evaluating an ideal fall detection for a wrist-worn configuration. With this purpose, the best result was achieved when the method K-Nearest Neighbors was employed, considering data from three IMU sensors: accelerometer, gyroscope and magnetometer. In this situation, an ideal sensitivity and a high specificity (97.9%) were achieved, leading to an accuracy of 99%.

Thus, the objectives of this work were all achieved, as follows:

- The behavior of elderly people wrist movements was studied, allowing its spatial orientation estimation by accelerometer, gyroscope and magnetometer data;
- A database considering fall and non-fall simulation events was properly prepared, which was important for the development and evaluation of different fall detection algorithms;
- Different IMU variables and configurations were evaluated, making possible the definition of the best case for each approach;
- The movement decomposition between vertical and non-vertical movements was evaluated, and its relevance was evidenced mainly for threshold based algorithms;
- Two threshold based algorithms were developed, and the best achieved accuracy was 91.1% for this approach;
- The achieved results for the threshold based algorithms were confronted with the results obtained with machine learning methods, allowing a proper comparison about both approaches;
- The best fall detection algorithm for a wrist worn device was defined as the one based on the K-Nearest Neighbors machine learning method: 99% of accuracy. This result allowed the achievement of the work general objective.

The results achieved by the machine learning methods were considerably higher than those achieved by the threshold-based algorithms. After evaluating many different algorithms possibilities, this work concludes that machine learning approaches are potentially able to achieve ideal results for a fall detection system based on a wrist-worn device, while threshold-based algorithms are not able to achieve the same results, at least without requiring extremely high sampling rates and complex algorithms to extract information from IMU sensors.

The exhaustive analysis of different methods for fall detection solutions based on wrist-worn devices (which is not a common wearable configuration in literature), followed by the conclusion of machine learning methods as a robust approach for their development, contributes significantly to the research and development of these solutions, which allow to improve and save elderly people lives.

## 5.1 FUTURE WORK

The next steps of this work are related to a deeper evaluation of machine learning algorithms for fall detection. For this, different combinations of IMU sensors data must be evaluated, identifying the best configuration which requires less data and computing resources.

Furthermore, a more extensive data acquisition protocol must be proposed, involving additional non-fall activities (e.g. lying down and standing up, taking a shower) and different fall events (e.g. leaning against a wall and then slipping vertically). Also, 24-hours monitoring tests are necessary, in order to evaluate the system behavior during a long period of time.

Finally, the development of the notification system must be done to define a complete solution for elderly falls, including a fall detection wrist-worn device and a notification system for an immediate help response to elderly people .

# REFERENCES


ABREU, H. C. d. A. et al. Incidence and predicting factors of falls of older inpatients. **Revista de Saúde Pública**, v. 49, p. 13–20, 2015. ISSN 1518-8787.

AL-AAMA, T. Falls in the elderly: spectrum and prevention. **Canadian family physician**, v. 57, n. 7, p. 771–6, jul 2011. ISSN 1715-5258.

Analog Devices Inc. **ADXL345 Datasheet**. 2009. 1–40 p.

ANDO, B. et al. A Multisensor Data-Fusion Approach for ADL and Fall classification. **IEEE Transactions on Instrumentation and Measurement**, v. 65, n. 9, p. 1960–1967, sep 2016. ISSN 0018-9456.

ASCHKENASY, M. T.; ROTHENHAUS, T. C. Trauma and Falls in the Elderly. **Emergency Medicine Clinics of North America**, v. 24, n. 2, p. 413–432, may 2006. ISSN 07338627.

AZIZ, O. et al. A comparison of accuracy of fall detection algorithms (threshold-based vs. machine learning) using waist-mounted tri-axial accelerometer signals from a comprehensive set of falls and non-fall trials. **Medical & Biological Engineering & Computing**, Springer Berlin Heidelberg, v. 55, n. 1, p. 45–55, jan 2017. ISSN 0140-0118.

BAGNASCO, A.; SCAPOLLA, A. M.; SPASOVA, V. Design, implementation and experimental evaluation of a wireless fall detector. In: **Proceedings of the 4th International Symposium on Applied Sciences in Biomedical and Communication Technologies - ISABEL '11**. New York, New York, USA: ACM Press, 2011. p. 1–5. ISBN 9781450309134.

BALDONI, A. O.; PEREIRA, L. R. L. O impacto do envelhecimento populacional Brasileiro para o sistema de saúde sob a óptica da farmacoepidemiologia: Uma revisão narrativa. **Revista de Ciencias Farmaceuticas Basica e Aplicada**, v. 32, n. 3, p. 313–321, 2011. ISSN 18084532.

BENNETT, T. R. et al. Inertial Measurement Unit-Based Wearable Computers for Assisted Living Applications: A signal processing perspective. **IEEE Signal Processing Magazine**, v. 33, n. 2, p. 28–35, 2016. ISSN 1053-5888.

BIANCHI, F. et al. Barometric pressure and triaxial accelerometry-based falls event detection. **IEEE Transactions on Neural Systems and Rehabilitation Engineering**, v. 18, n. 6, p. 619–627, 2010. ISSN 15344320.

BISHOP, C. M. **Neural Networks for Pattern Recognition**. [S.l.]: Oxford University Press, 1995.

BOULTON, E. et al. Developing the FARSEEING Taxonomy of Technologies: Classification and description of technology use (including ICT) in falls prevention studies. **Journal of Biomedical Informatics**, Elsevier Inc., v. 61, p. 132–140, 2016. ISSN 15320464.

BOURKE, A.; O'BRIEN, J.; LYONS, G. Evaluation of a threshold-based tri-axial accelerometer fall detection algorithm. **Gait & Posture**, v. 26, n. 2, p. 194–199, jul 2007. ISSN 09666362.

CHACCOUR, K. et al. From Fall Detection to Fall Prevention: A Generic Classification of Fall-Related Systems. **IEEE Sensors Journal**, v. 17, n. 3, p. 1–1, 2016. ISSN 1530-437X.

CHEFFENA, M. Fall Detection Using Smartphone Audio Features. **IEEE Journal of Biomedical and Health Informatics**, v. 20, n. 4, p. 1073–1080, 2016. ISSN 21682194.

CHENG, W.-C.; JHAN, D.-M. Triaxial accelerometer-based fall detection method using a self-constructing cascade-AdaBoost-SVM classifier. **IEEE Journal of Biomedical and Health Informatics**, v. 17, n. 2, p. 411–419, 2013. ISSN 21682194.

CHERKASSKY, V.; MULIER, F. F. **Learning from Data: Concepts, Theory and Methods**. [S.l.]: Wiley, 1998.

CONCEPCION, M. A. A. et al. Mobile activity recognition and fall detection system for elderly people using Ameva algorithm. **Pervasive and Mobile Computing**, Elsevier B.V., v. 34, p. 3–13, 2016. ISSN 15741192.

DAHER, M. et al. Elder Tracking and Fall Detection System using Smart Tiles. **IEEE Sensors Journal**, v. 17, n. c, p. 1–1, 2016. ISSN 1530-437X.

DATASUS. **Morbidade Hospitalar do SUS**. 2015. Disponível em: <http://tabnet.datasus.gov.br/cgi/tabcgi.exe?sih/cnv/ni%0Auf.def>.

DEGEN, T. et al. SPEEDY:a fall detector in a wrist watch. In: **Seventh IEEE International Symposium on Wearable Computers**. [S.l.]: IEEE, 2003. p. 184–187. ISBN 0-7695-2034-0.

DUIN, R. P. W.; PEKALSKA, E. Pattern Recognition : Introduction and Terminology. p. 77, 2016.

FAWCETT, T. An introduction to ROC analysis. **Pattern Recognition Letters**, v. 27, n. 8, p. 861–874, jun 2006. ISSN 01678655.

FERREIRA, D. C. d. O.; YOSHITOME, A. Y. Prevalência e caraterísticas das quedas de idosos institucionalizados. **Revista Brasileira de Enfermagem**, v. 63, n. 6, p. 991–997, dec 2010. ISSN 0034-7167.

GANANÇA, F. F. et al. Circunstâncias e conseqüências de quedas em idosos com vestibulopatia crônica. **Revista Brasileira de Otorrinolaringologia**, v. 72, n. 3, p. 388–393, jun 2006. ISSN 0034-7299.

GARRIPOLI, C. et al. Embedded DSP-based telehealth radar system for remote in-door fall detection. **IEEE Journal of Biomedical and Health Informatics**, v. 19, n. 1, p. 92–101, 2015. ISSN 21682194.

GOLDSTEIN, H.; POOLE, C.; SAFKO, J. **Classical Mechanics**. 2nd edition. ed. [S.l.: s.n.], 2007. ISBN 0201657023.

GUIMARÃES, J. M. N.; FARINATTI, P. d. T. V. Análise descritiva de variáveis teoricamente associadas ao risco de quedas em mulheres idosas. **Revista Brasileira de Medicina do Esporte**, v. 11, n. 5, p. 299–305, oct 2005. ISSN 1517-8692.

GURLEY, R. J. et al. Persons Found Helpless in Their Homes. **New England Journal of Medicine**, v. 334, n. 26, p. 1710–1716, nov 1996. ISSN 0028-4793.

HAYES, D. L. et al. INTERFERENCE WITH CARDIAC PACEMAKERS BY CELLULAR TELEPHONES. **The New England Journal Of Medicine**, v. 336, n. 21, p. 1473–1479, 1997.

HAYKIN, S. **Neural Networks: A Comprehensive Foundation**. [S.l.]: Prentice Hall, 1998.

HONEYWELL. **HMC5883L Datasheet**. 2010. 20 p.

IGUAL, R.; MEDRANO, C.; PLAZA, I. Challenges, issues and trends in fall detection systems. **BioMedical Engineering OnLine**, v. 12, n. 1, p. 66, 2013. ISSN 1475-925X.

KAMBHAMPATI, S. S. et al. Unified framework for triaxial accelerometer-based fall event detection and classification using cumulants and hierarchical decision tree classifier. **Healthcare Technology Letters**, v. 2, n. 4, p. 101–107, aug 2015. ISSN 2053-3713.

KANG, J. M.; YOO, T.; KIM, H. C. A wrist-worn integrated health monitoring instrument with a tele-reporting device for telemedicine and telecare. **IEEE Transactions on Instrumentation and Measurement**, v. 55, n. 5, p. 1655–1661, 2006. ISSN 00189456.

KANGAS, M. et al. Determination of simple thresholds for accelerometry-based parameters for fall detection. In: **2007 29th Annual International Conference of the IEEE Engineering in Medicine and Biology Society**. Lyon, France: IEEE, 2007. v. 2007, p. 1367–1370. ISBN 978-1-4244-0787-3. ISSN 1557-170X.

KHAN, S. S.; HOEY, J. Review of Fall Detection Techniques: A Data Availability Perspective. Elsevier Ltd, v. 39, p. 12–22, 2016. ISSN 13504533.

KOWNACKI, C. Optimization approach to adapt Kalman filters for the real-time application of accelerometer and gyroscope signals' filtering. **Digital Signal Processing**, v. 21, n. 1, p. 131–140, jan 2011. ISSN 10512004.

KUIPERS, J. **Quaternions and Rotation Sequences: A Primer with Applications to Orbits, Aerospace, and Virtual Reality**. [S.l.]: Princeton University Press, 2002. (Princeton paperbacks). ISBN 9780691102986.

KWOLEK, B.; KEPSKI, M. Human fall detection on embedded platform using depth maps and wireless accelerometer. **Computer Methods and Programs in Biomedicine**, v. 117, n. 13, p. 489–501, 2014. ISSN 0169-2607.

LATASH, M. L. et al. Movement sway: changes in postural sway during voluntary shifts of the center of pressure. **Experimental Brain Research**, v. 150, n. 3, p. 314–324, jun 2003. ISSN 0014-4819.

LAZZARETTI, A. E. **Segmentação, classificação e detecção de novas classes de eventos em oscilografias de redes de distribuição de energia elétrica**. 220 p. Tese (Doutorado) — Universidade Tecnológica Federal do Paraná, 2015.

LEE, J. K.; ROBINOVITCH, S. N.; PARK, E. J. Inertial Sensing-Based Pre-Impact Detection of Falls Involving Near-Fall Scenarios. **IEEE Transactions on Neural Systems and Rehabilitation Engineering**, v. 23, n. 2, p. 258–266, 2015. ISSN 15344320.

LIU, J.; LOCKHART, T. E. Development and evaluation of a prior-to-impact fall event detection algorithm. **IEEE Transactions on Biomedical Engineering**, v. 61, n. 7, p. 2135–2140, 2014. ISSN 15582531.

LOPES, M. C. D. L. et al. FATORES DESENCADEANTES DE QUEDAS NO DOMICÍLIO EM UMA COMUNIDADE DE IDOSOS. **Cogitare Enfermagem**, v. 12, n. 4, p. 472–477, dec 2007.

MADGWICK, S. O. H.; HARRISON, A. J. L.; VAIDYANATHAN, R. Estimation of IMU and MARG orientation using a gradient descent algorithm. In: **2011 IEEE International Conference on Rehabilitation Robotics**. [S.l.]: IEEE, 2011. p. 1–7. ISBN 978-1-4244-9862-8. ISSN 19457898.

MAZO, G. et al. Condições de saúde, incidência de quedas e nível de atividade física dos idosos. **Revista Brasileira de Fisioterapia**, v. 11, n. 6, p. 437–442, dec 2007. ISSN 1413-3555.

Miao Yu et al. An Online One Class Support Vector Machine-Based Person-Specific Fall Detection System for Monitoring an Elderly Individual in a Room Environment. **IEEE Journal of Biomedical and Health Informatics**, v. 17, n. 6, p. 1002–1014, nov 2013. ISSN 2168-2194.

MUBASHIR, M.; SHAO, L.; SEED, L. A survey on fall detection: Principles and approaches. **Neurocomputing**, Elsevier, v. 100, p. 144–152, 2013. ISSN 09252312.

NOURY, N. et al. A proposal for the classification and evaluation of fall detectors. **IRBM**, v. 29, n. 6, p. 340–349, dec 2008. ISSN 19590318.

OZCAN, K. et al. Automatic Fall Detection and Activity Classification by a Wearable Embedded Smart Camera. **IEEE Journal on Emerging and Selected Topics in Circuits and Systems**, Springer New York, New York, NY, v. 3, n. 2, p. 125–136, jun 2013. ISSN 2156-3357.

OZCAN, K.; VELIPASALAR, S.; VARSHNEY, P. K. Autonomous Fall Detection With Wearable Cameras by Using Relative Entropy Distance Measure. **IEEE Transactions on Human-Machine Systems**, v. 47, n. 1, p. 1–9, 2016. ISSN 2168-2291.

PANNURAT, N.; THIEMJARUS, S.; NANTAJEEWARAWAT, E. Automatic Fall Monitoring: A Review. **Sensors**, v. 14, n. 7, p. 12900–12936, jul 2014. ISSN 1424-8220.

PANNURAT, N.; THIEMJARUS, S.; NANTAJEEWARAWAT, E. A Hybrid Temporal Reasoning Framework for Fall Monitoring. **IEEE Sensors Journal**, v. 17, n. 6, p. 1749–1759, 2017. ISSN 1530-437X.

PERRY, J. T. et al. Survey and evaluation of real-time fall detection approaches. In: **2009 6th International Symposium on High Capacity Optical Networks and Enabling Technologies (HONET)**. [S.l.]: IEEE, 2009. p. 158–164. ISBN 978-1-4244-5992-6.

PIERLEONI, P. et al. A Wearable Fall Detector for Elderly People Based on AHRS and Barometric Sensor. **IEEE Sensors Journal**, v. 16, n. 17, p. 6733–6744, sep 2016. ISSN 1530-437X.

PIERLEONI, P. et al. A High Reliability Wearable Device for Elderly Fall Detection. **IEEE Sensors Journal**, v. 15, n. 8, p. 4544–4553, 2015. ISSN 1530437X.

QUADROS, T. de; LAZZARETTI, A. E.; SCHNEIDER, F. K. Detecção de quedas em idosos utilizando dispositivo localizado no pulso. In: **XXV Congresso Brasileiro de Engenharia Biomédica – CBEB 2016**. [S.l.: s.n.], 2016.

QUADROS, T. de; LAZZARETTI, A. E.; SCHNEIDER, F. K. Development and Evaluation of a Method for Fall Detection Based on a Wrist-Located Device. In: . [S.l.: s.n.], 2017. p. 256–259.

REISS, A.; STRICKER, D. Creating and benchmarking a new dataset for physical activity monitoring. In: **The 5th Workshop on Affect and Behaviour Related Assistance (ABRA)**. [S.l.]: ACM Press, 2012.

RUWER, S. L.; ROSSI, A. G.; SIMON, L. F. Equilíbrio no idoso. **Revista Brasileira de Otorrinolaringologia**, v. 71, n. 3, p. 298–303, jun 2005. ISSN 0034-7299.

SABATINI, A. M. et al. Prior-to- and Post-Impact Fall Detection Using Inertial and Barometric Altimeter Measurements. **IEEE Transactions on Neural Systems and Rehabilitation Engineering**, v. 24, n. 7, p. 774–83, 2016. ISSN 1558-0210.

SRI-ON, J. et al. Revisit, Subsequent Hospitalization, Recurrent Fall, and Death Within 6 Months After a Fall Among Elderly Emergency Department Patients. **Annals of Emergency Medicine**, American College of Emergency Physicians, v. 70, n. 4, p. 516–521.e2, oct 2017. ISSN 01960644.

ST Microelectronics. **L3G4200D Datasheet**. 2010. 42 p.

STONE, E. E.; SKUBIC, M. Fall detection in homes of older adults using the Microsoft Kinect. **IEEE Journal of Biomedical and Health Informatics**, v. 19, n. 1, p. 290–301, 2015. ISSN 2168-2194.

STRICKLAND, J. **What is a gimbal – and what does it have to do with NASA?** 2008. Disponível em: <http://science.howstuffworks.com/gimbal1.htm>.

TINETTI, M. E.; SPEECHLEY, M.; GINTER, S. F. Risk Factors for Falls among Elderly Persons Living in the Community. **New England Journal of Medicine**, v. 319, n. 26, p. 1701–1707, dec 1988. ISSN 0028-4793.

TONG, L. et al. HMM-based human fall detection and prediction method using tri-axial accelerometer. **IEEE Sensors Journal**, v. 13, n. 5, p. 1849–1856, 2013. ISSN 1530437X.

UICKER, J. J.; PENNOCK, G. R.; SHIGLEY, J. E. **Theory of Machines and Mechanisms**. 3rd edition. ed. New York, USA: Oxford University Press, 2003. 1709 p. ISBN 978-0195371239.

UNITED NATIONS. World Population Ageing 2015. **Department of Economic and Social Affairs, Population Division**, New York, USA, n. ST/ESA/SER.A/390, p. 164, 2015.

VALCOURT, L.; De La Hoz, Y.; LABRADOR, M. Smartphone-based Human Fall Detection System. **IEEE Latin America Transactions**, v. 14, n. 2, p. 1011–1017, 2016. ISSN 15480992.

WANG, C. et al. A Low-Power Fall Detector using Triaxial Accelerometry and Barometric Pressure Sensing. **IEEE Transactions on Industrial Informatics**, v. 12, n. 6, p. 2302–2311, 2016. ISSN 1551-3203.

WHO, W. H. O. **WHO Global Report on Falls Prevention in Older Age.** Victoria, Canada, 2007. 53 p.

WHO, W. H. O. **World Report on Ageing and Health**. Luxembourg: World Health Organization, 2015. 246 p. (Nonserial Publication). ISBN 9789241565042.

WU, G. Distinguishing fall activities from normal activities by velocity characteristics. **Journal of Biomechanics**, v. 33, n. 11, p. 1497–1500, nov 2000. ISSN 00219290.

YOUNG, W. R.; Mark Williams, A. How fear of falling can increase fall-risk in older adults: Applying psychological theory to practical observations. **Gait & Posture**, Elsevier B.V., v. 41, n. 1, p. 7–12, jan 2015. ISSN 09666362.

YUAN, J. et al. Power-efficient interrupt-driven algorithms for fall detection and classification of activities of daily living. **IEEE Sensors Journal**, v. 15, n. 3, p. 1377–1387, 2015. ISSN 1530437X.